Copper availability governs nitrous oxide accumulation in wetland soils and stream sediments

Neha Sharma,[1] Elaine D. Flynn,[2] Jeffrey G. Catalano[2] and Daniel E. Giammar[1*]

[1]*Department of Energy, Environmental and Chemical Engineering, Washington University in St. Louis, St. Louis, Missouri 63130, United States*

[2]*Department of Earth and Planetary Sciences, Washington University in St. Louis, St. Louis, Missouri 63130, United States*

*Corresponding Author:
Address: Department of Energy, Environmental and Chemical Engineering, Washington University in St. Louis, St. Louis, MO 63130, USA
Phone: (314) 935-6849
Email: giammar@wustl.edu

Submitted to *Geochimica et Cosmochimica Acta*

ABSTRACT

Denitrification is microbially-mediated through enzymes containing metal cofactors. Laboratory studies of pure cultures have highlighted that the availability of Cu, required for the multicopper enzyme nitrous oxide reductase, can limit N_2O reduction. However, in natural aquatic systems, such as wetlands and hyporheic zones in stream beds, the role of Cu in controlling denitrification remains incompletely understood. In this study, we collected soils and sediments from three natural environments -- riparian wetlands, marsh wetlands, and a stream -- to investigate their nitrogen species transformation activity at background Cu levels and different supplemented Cu loadings. All of the systems displayed low solid-phase associated Cu (40 - 280 nmol g^{-1}), which made them appropriate sites for evaluating the effect of limited Cu availability on denitrification. In laboratory incubation experiments, high concentrations of N_2O accumulated in all microcosms lacking Cu amendment except for one stream sediment sample. With Cu added to provide dissolved concentrations at trace levels (10-300 nM), reduction of N_2O to N_2 in the wetland soils and stream sediments was enhanced. A kinetic model could account for the trends in nitrogen species by combining the reactions for microbial reduction of NO_3^- to $NO_2^-/N_2O/N_2$ and abiotic reduction of NO_2^- to N_2. The model revealed that the rate of N_2O to N_2 conversion increased significantly in the presence of Cu. For riparian wetland soils and stream sediments, the kinetic model also suggested that overall denitrification is driven by abiotic reduction of NO_2^- in the presence of inorganic electron donors. This study demonstrated that natural aquatic systems containing Cu at concentrations less than or equal to crustal abundances may display incomplete reduction of N_2O to N_2 that would cause N_2O accumulation and release to the atmosphere.

Keywords: wetlands, hyporheic zone, denitrification, nitrous oxide, copper, bioavailability, organic carbon

1. Introduction

Nitrous oxide (N_2O) is a potent greenhouse gas whose global warming potential per unit mass is 265–298 times that of carbon dioxide (CO_2) for a 100-year timescale (IPCC, 2014; Sovacool et al., 2021). Global N_2O emissions in the decade between 2007-2016 averaged 17 Tg N yr^{-1}, of which 57% (9.7 Tg N yr^{-1}) were contributed by natural soils and oceans (Tian et al., 2020). Denitrification, an anoxic process in which nitrate (NO_3^-) is reduced to N_2, is a key biogeochemical process that regulates the amount of N_2O released from both terrestrial and aquatic ecosystems into the atmosphere (Makowski, 2019; Tian et al., 2020; Martinez-Espinosa et al., 2021). Natural aquatic systems, especially those that display vertical redox gradients, such as wetlands and hyporheic zones in streams, are active sites for denitrification (Merill and Tonjes, 2014; Nag et al., 2017; Mwagona et al., 2019; Martinez-Espinosa et al., 2021). Oxic regions above redox transition zones favor the oxidation of ammonia (NH_3) to NO_3^- via nitrification, and the anoxic regions below redox transition zones promote denitrification with NO_3^- being reduced to nitrite (NO_2^-), nitric oxide (NO), N_2O, and N_2. The incomplete conversion of NO_3^- and NO_2^- to N_2 causes N_2O to be released from the aquatic systems to the atmosphere.

An array of metalloenzymes that contain Fe, Cu, and Mo are involved in reducing nitrate and intermediate species to N_2 during denitrification (Godden et al., 1991; Bertero et al., 2003; Nojiri et al., 2007). The transformation of NO_3^- to NO_2^- is catalyzed by respiratory nitrate reductase (Nar), which requires Fe and Mo for complete conversion (Bertero et al., 2003; Jormakka et al., 2004). Depending on the type of microorganism, reduction of NO_2^- to NO is catalyzed by either an iron-containing nitrite reductase (NirS) or a Cu-containing nitrite reductase (NirK) (Godden et al., 1991; Nojiri et al., 2007). NO is rapidly transformed to N_2O with an Fe-bearing nitric oxide reductase (cNOR), and in the final step, N_2O is reduced to N_2 by a Cu-rich nitrous oxide reductase (Nos) (Brown et al., 2000).

A scarcity of available Cu can limit the conversion of N_2O to N_2. Laboratory studies of pure cultures have demonstrated that Cu limitation resulted in N_2O accumulation (Iwasaki et al., 1980; Granger and Ward, 2003; Black et al., 2016). Granger and Ward (2003) conducted a study with *Pseudomonas stutzeri* and

Paracoccus denitrificans in an artificial seawater medium to evaluate the effect of Cu on denitrification. They observed that Cu concentrations of approximately 3 nM caused N_2O to accumulate, whereas 10 nM Cu resulted in increased growth rates and complete conversion of N_2O to N_2. The growth of two denitrifying microorganisms, *Alcaligenes* sp. NGIB 11015 and *Alcaligenes faecalis* lAM 1015, was also stimulated by the addition of Cu in the range of 0.5 to 40 µM (Iwasaki et al., 1980). Another study on *P. stutzeri* revealed that when dissolved Cu concentrations were varied between 0- 80 µM, the maximum conversion of N_2O to N_2 was achieved at a concentration of 0.80 µM (Black et al., 2016).

In soils and sediments, high concentrations of Cu can inhibit denitrification, whereas low availability of Cu can limit microbial activity causing accumulation of intermediate nitrogen species. In estuarine sediments, the addition of 79 µg g^{-1} Cu inhibited microbial activity by 85% and specifically increased the accumulation of NO_2^- and N_2O (Magalhaes et al., 2007). Similarly, the addition of Cu at high loadings of 250-1000 µg g^{-1} increased N_2O emissions from soils and wetland sediments (Sakadevan et al., 1999; Shaaban et al., 2019). In these three studies, the associated dissolved Cu concentrations were not measured. While the three studies just noted had increased accumulation of N_2O associated with high Cu, two other studies found that the addition of Cu to systems with initially low Cu decreased N_2O accumulation. A recent study of freshwater wetland sediments that initially had 37.8 µg g^{-1} Cu and were amended with $CuSO_4$ to have 26 µM dissolved Cu showed an increased abundance of nitrite and nitrous oxide reductase genes that enhanced the conversion of N_2O to N_2 (Giannopoulos et al., 2020). Similarly, a study of freshwater sediments collected from central Indiana also showed that N_2O accumulation decreased when the sediments were amended with 50-100 µg g^{-1} Cu (Jacinthe and Tedesco, 2009). On the other hand, the addition of 100 µg L^{-1} Cu did not have any effect on N_2O emissions release in freshwater wetland sediments (Doroski et al., 2019). Copper concentrations in uncontaminated environments are typically low (Black et al., 2011; Black et al., 2016), and hence limited Cu bioavailability in such settings may significantly affect N_2O conversion via denitrification.

In natural aquatic systems, the relationship between the total Cu amount in the sediments and the bioavailable concentration of dissolved Cu is controlled by the presence of solid phases, such as sulfide

minerals, particulate organic carbon, iron and manganese oxyhydroxides, and clay minerals (Du Laing et al., 2009; Campana et al., 2012; Bourgeault et al., 2013; Zhang et al., 2014). Changes in aquatic phase parameters, including pH, redox potential, and the concentration of ligands, can mobilize/immobilize metals from solid phases, thus affecting their bioavailability (Du Laing et al., 2009; Zhang et al., 2014). Dissolved Cu is present as a free hydrated ion (Cu^{2+}) and complexes with hydroxides, inorganic ligands (carbonates and chlorides), and organic ligands (humic and fulvic acids) depending on the water composition (Kozelka and Bruland, 1998). Strong organic Cu-chelates, such as complexes with humic acids and fulvic acids, are inert and hence not readily bioavailable, but inorganic hydroxy and carbonate complexes are labile and might be toxic to some microorganisms at concentrations as low as 10 µg L^{-1} (Allen and Hansen, 1996; Bruland et al., 2000; Huang and Wang, 2003; Bourgeault et al., 2013). Several studies have reported that Cu has a high affinity for dissolved organic carbon and exists predominantly as Cu-organic ligand complexes in natural waters (Skrabal et al., 2000; Chakraborty et al., 2015; Ren et al., 2015; Waska et al., 2019). Thus, even dissolved Cu concentrations that would be expected to be optimal for N_2O conversion (>10 nM) might exert a limiting effect on denitrification in natural environments if the Cu is predominantly complexed in non-bioavailable forms.

In natural environments, nitrogen cycling can also occur via processes other than biological denitrification. These processes include dissimilatory nitrate reduction to ammonium (DNRA), anaerobic ammonium oxidation (anammox), chemoautotrophic denitrification, and abiotic photochemical and thermochemical processes (Burgin and Hamilton, 2007; Doane, 2017; Martinez-Espinosa et al., 2021). Other elemental cycles, such as those of iron and sulfur, play important roles in nitrogen cycling in natural environments. Autotrophic and mixotrophic denitrifiers can gain energy from mediating the reduction of NO_3^- by inorganic electron donors that include sulfur compounds (S^o, S^{2-}, $S_2O_3^{2}$), pyrite (FeS_2), Fe^{2+}, Fe^0, and Mn^{2+} (Davidson et al., 2003; Weber et al., 2006; Melton et al., 2014; Di Capua et al., 2019; Wei et al., 2019). Additionally, abiotic reduction of NO_3^-/NO_2^- by dissolved Fe(II) or Fe(II)-bearing minerals has been studied extensively as a pathway for N_2O or N_2 formation under anoxic conditions (Moraghan and Buresh, 1977; Ottley et al., 1997; Matocha et al., 2012; Melton et al., 2014; Peters et al., 2014; Buchwald et al.,

2016; Liu et al., 2019; Matus et al., 2019; Chen et al., 2020). Fe(II)-rich flooded soils showed decreased N_2O emissions because high Fe(II) concentrations favored the complete conversion of NO_3^- to N_2 (Wang et al., 2016). A recent study of marine sediments found that ~15-25% of the total N_2O released was produced by abiotic nitrite reduction in the presence of Fe(II) (Otte et al., 2019).

The effects of redox conditions, substrate availability, temperature, and pH on denitrification have been widely studied (Nowicki, 1994; Koponen et al., 2004; Baeseman et al., 2006; Nag et al., 2017). There has also been significant progress in understanding the toxic effects of elevated Cu levels on the denitrification pathway, but only limited studies have investigated the effect of Cu availability on N_2O accumulation in uncontaminated aquatic systems (Twining et al., 2007; Giannopoulos et al., 2020). A broader understanding of how Cu affects N-cycling in natural systems can improve the accuracy of ecosystem models, such as the Dynamic Land Ecosystem Model (DLEM) (Tian et al., 2020), used to estimate N_2O emissions. The objectives of this study were to (1) investigate the effect of trace concentrations of dissolved Cu on nitrate reduction and the formation of reaction products (NO_2^- and N_2O) with soils and sediments from three different natural aquatic systems and (2) develop a kinetic model for the denitrification reactions that can quantify the effect of Cu addition on the transformation and accumulation of nitrogen species in environmental systems.

2. Materials and methods

2.1 Description of sites

To investigate the effect of Cu on denitrification, we selected three separate natural aquatic systems: marsh wetlands at Argonne National Laboratory (ANL) in Lemont, Illinois; riparian wetlands in the Tims Branch (TB) watershed at the Savannah River Site in Aiken County, South Carolina; and East Fork Poplar Creek (EFPC) at Oak Ridge National Laboratory (ORNL) in Oak Ridge, Tennessee. Detailed information on the sampling sites, sampling techniques, and soil characterization can be found in our recent study on trace metal speciation at these sites (Yan et al., 2021). Briefly, soil/sediment and surface water samples were collected from two different locations at each aquatic system. To identify locations within the sites, we used

the labels “Riparian 1” and “Riparian 2” for Tims Branch riparian wetland soils; “Stream 1” and “Stream 2” for Oak Ridge stream sediment sites, and “Marsh 1” and “Marsh 2” for Argonne marsh wetland soils.

2.2 Sampling and characterization

Soil or sediment cores were collected in polycarbonate tubes. Cores from the marsh wetland and riparian wetland were shipped on ice to Washington University in St. Louis, where they were extruded from the tubes and immediately transferred to an anaerobic chamber (Coy Laboratory Products, 3% H_2/97% N_2, with Pd catalyst) to maintain anaerobic conditions. The cores from the stream sediment site were extruded at ORNL within 1 h of sampling, impulse sealed in polyethylene pouches in an anaerobic chamber, and stored in a refrigerator at 4°C before being shipped on ice to Washington University, where they were stored in an anaerobic chamber.

Surface water samples were filtered using 0.22 µm mixed cellulose ester (MCE) syringe filters. A portion was immediately acidified to 2% nitric acid (HNO_3), and the rest of the filtered water was stored at 4 °C prior to anion and nutrient analysis. The acidified surface water samples were analyzed to quantify the dissolved major elements (sodium, magnesium, aluminum, silicon, potassium, and calcium) and trace metals (cobalt, nickel, copper, and zinc). The major elements were quantified using a Thermo Scientific iCap 7400 Duo inductively-coupled plasma optical emission spectrometer (ICP-OES), and the trace metals were quantified with an inductively coupled plasma mass spectrometer (PerkinElmer Elan DRC II). The unacidified water samples were used to measure the concentrations of dissolved anions (Br^-, Cl^-, F^-, and SO_4^{2-}) using a Thermo Scientific Dionex Integrion high-pressure ion chromatograph (IC) with a conductivity detector. The major elements and trace metals were extracted from the soils/sediments by microwave-assisted digestion and were analyzed using ICP-OES and ICP-MS, respectively (Yan et al., 2021). The extractable nutrients (nitrate, ammonium, and phosphate) in the soils and sediments were obtained using a 2 M potassium chloride extraction method adapted from previous studies (Sparks et al., 1996; Pansu and Gautheyrou, 2006) and were measured using a Seal Analytical AQ300 Discrete Multi-Chemistry Analyzer.

2.3 Reagent preparation

All the solutions were prepared in an anaerobic chamber (3% H_2/97% N_2, with Pd catalyst) using deoxygenated deionized water (>18.2 MΩ cm). Deoxygenated water was prepared by bubbling N_2 gas through it for 4-5 h, followed by bubbling the water in an anaerobic chamber for 3 h with a filtered stream of the anaerobic chamber atmosphere that had been passed in sequence through solutions of ferrous chloride and KOH to remove traces of oxygen and carbon dioxide. A colorimetric assay (CHEMets test kit K-7511) was used to ensure that the dissolved oxygen level in the deoxygenated water was below the detection limit (2 µg/L). Copper chloride dihydrate (99.99%, Sigma Aldrich) was used to vary the Cu loading in denitrification studies. All other salts (sodium chloride, potassium chloride, sodium sulfate, magnesium chloride hexahydrate, magnesium sulfate, calcium sulfate dihydrate, ammonium chloride, and disodium phosphate) used for preparing simulated site water were purchased from Thermo Fisher Scientific and were of reagent grade. Sodium nitrate and potassium nitrate (99.9%, Sigma Aldrich) were used for preparing a stock solution of nitrate. Nitric acid (trace metal grade, Thermo Fisher Scientific) was used to acidify samples for dissolved metal analysis. Reagents and calibration standards for nutrient analysis were prepared using reagent grade chemicals.

2.4 Laboratory incubation experiments

The incubation studies were conducted with the samples from the riparian wetlands (Riparian 2 and Riparian 1), the stream (Stream 2 and Stream 1) and the marsh wetlands (Marsh 1). The two locations in riparian wetland soils and stream sediments had different total carbon, sulfur, and metal contents and exhibited different solid-phase speciation of Cu. Both the locations in the marsh wetland soils showed similar characteristics (Yan et al., 2021), so the samples from only one marsh wetland location (Marsh 1) were used in further studies. Cu uptake experiments were performed to determine the Cu concentration range to consider in the incubation studies. The soils and sediments were completely homogenized before uptake experiments. These experiments were conducted in 15 mL polypropylene tubes containing 1-200 µM $CuCl_2$ and 10 mL of simulated site water, maintained at the desired pH (5.0 for Riparian 1 and Riparian

2, 7.6 for Stream 1 and Stream 2, and 7.0 for Marsh 1) and 0.5 g of soil/sediment. The recipe for the simulated water included the major cations and anions analyzed in the water samples (Table S1 in the Supplementary material). Samples were rotated end-over-end for 24 h to ensure complete mixing. After 4 h and 8 h of rotation, the pH values were readjusted to the original values, using 1M NaOH and 2M HCl solutions. The suspension was then immediately filtered using disposable 0.22 µm MCE syringe filters and acidified to 1% HNO_3. Dissolved Cu concentrations were measured by ICP-MS (PerkinElmer, NexION 2000).

Incubation experiments were initiated under anaerobic conditions in 100 mL serum bottles containing 2.5 g of homogenized soil/sediment along with 50 mL of simulated site water. The pH of the slurries was adjusted to 5.0 for Riparian 1 and Riparian 2, 7.6 for Stream 1 and Stream 2, and 7.0 for Marsh 1, using NaOH and HCl solutions. For each site, three different conditions were studied: no Cu added (control), low Cu loading, and high Cu loading (loading details are in Table 1). The different Cu loadings were selected based on the Cu uptake experiments discussed above. The selection of loadings was done so that the dissolved concentrations after 24 h of equilibration ranged between 10-30 nM and 500-1000 nM for low and high Cu loadings, respectively (Figure 1 and Table 1). After 24 h of equilibration, 1 mM NO_3^- was added, and the bottles were sealed with a 20 mm butyl stopper and aluminum cap. Immediately after the addition of NO_3^-, 1 mL of the fluid was sampled to determine the concentrations of dissolved metals and nutrients. The bottles were removed from the anaerobic chamber after NO_3^- addition and were flushed for 10 minutes with ultrapure N_2 to remove trace amounts of O_2 and H_2 from the headspace.

To determine N_2O concentrations, headspace gas samples were taken from each serum bottle at 24 h intervals and were transferred to 3 mL pre-evacuated glass vials (Exetainer®, Labco, United Kingdom) using a gas-tight syringe. The vials were stored upside down to prevent gas leakage from the septum. N_2O concentrations in the samples were measured using a gas chromatograph (GC) (Thermo Scientific GC TRACE 1310). Specifically, 1000 µL of the gas sample was injected (split injection at the split rate of 10:1) into the GC inlet (heated to 130 °C) using a TriPlus RSH (Thermo Scientific) autosampler equipped with a 2500 µL headspace syringe. The temperature of the column (Supelco Carboxen 1010 PLOT, 30 m x 0.32

mm) was maintained at 50 °C for 7.5 min, after which it was ramped to 130 °C using a rate of 20 °C/min and then kept at this temperature for 2 min. Helium was used as the carrier gas at a flow rate of 30 mL/min. A pulse discharge detector (PDD) at 150 °C was used for the analysis of N_2O. The concentration of the standards varied from 10 ppmv to 0.1% N_2O and were prepared using a certified gas standard from Airgas. The concentration of N_2O dissolved in the fluid was determined using the ideal gas law and Henry's gas solubility law. The value of Henry's constant at 25 °C used for determining dissolved N_2O was $2.4*10^{-4}$ mol m^{-3} Pa^{-1} (Sander, 2015). The total N_2O present in the microcosm at the time of sampling was the sum of the gas in the headspace and the gas dissolved in the water.

To measure the dissolved phase constituents, 1 mL of slurry from each serum bottle was sampled and centrifuged (Spectrafuge 16M) for 5 min at 5000 rpm. To determine the dissolved metal (Cu, Fe, and Mn) concentrations, 300 µL of the supernatant was acidified to 1% HNO_3 and analyzed by ICP-MS. The remaining supernatant was divided to estimate the pH using Whatman pH indicator strips and to determine the nutrient concentrations (NO_3^-, NO_2^- and NH_4^+) spectrophotometrically using a discrete multi-chemistry analyzer (Seal Analytical AQ300). The samples used for nutrient analysis were frozen and then thawed overnight at 4°C before analysis. Nitrite was measured by the reaction of the sample with sulfanilamide in dilute phosphoric acid to form a diazonium compound which binds to N-(1-naphthyl)-ethylenediamine dihydrochloride to form an azo dye detected at 520 nm (Huffman and Barbarick, 1981). To determine the nitrate concentration, NO_3^- was first reduced to NO_2^- by cadmium and then the NO_2^- was measured. Ammonium present in the samples was determined by reacting the samples with hypochlorite liberated from dichloroisocyanurate in an alkaline solution followed by a reaction with salicylate in the presence of nitroferricyanide to form a blue indophenol dye, which was measured at 660 nm (Krom, 1980). At the end of incubation experiments, the final pH value was recorded using a pH electrode. The water was filtered and stored at 4°C to determine the dissolved organic carbon (DOC) concentration using a total organic carbon analyzer (Shimadzu TOC-L) at the end of incubation experiments.

2.5 Aqueous speciation of Cu

To estimate the speciation of Cu in the presence of organic carbon in the incubation experiments, the nonideal competitive adsorption-Donnan (NICA-Donnan) model in Visual MINTEQ 3.1 (Yan and Korshin, 2014) was used. The model is a combination of NICA which enables simulation of metal complexation to humic substances, and a Donnan model describing nonspecific electrostatic interactions between ions and humic substances (Benedetti et al., 1995; Benedetti et al., 1996; Ren et al., 2015). Although humic substances might not truly represent the dissolved organic matter present in aquatic systems (Kleber and Lehmann, 2019; Myneni, 2019), we used the NICA-Donnan model to estimate the aqueous speciation of Cu because this model has previously provided accurate predictions of metal speciation and availability in natural systems (Han et al., 2014; Ponthieu et al., 2016). NICA considers competitive binding between protons and metals to humic substances by accounting for binding site heterogeneity and ion-specific nonideality (Benedetti et al., 1995). The generic parameters obtained in previous studies for Cu and proton binding to humic material were used (Milne et al., 2001; Milne et al., 2003; Xu et al., 2016). Water chemistry parameters (pH, total dissolved elements (Table S1)), dissolved Cu, Fe, and Mn, and dissolved organic carbon (DOC) were used as the input parameters for determining dissolved Cu speciation. Three sets of conditions were used to account for Cu speciation at different total dissolved Cu concentrations corresponding to the control, low Cu loading, and high Cu loading experiments (details of the methodology in Section S1 in SM, Table S3). Under anoxic environments, as in our incubation experiments, Cu(II) can be reduced to Cu(I) by microorganisms, inorganic reductants, and redox-active functional groups on dissolved organic matter (Weber et al., 2006; Fulda et al., 2013b; Mehlhorn et al., 2018). Cu(I) can form stable complexes with inorganic ligands or thiol groups of organic matter (Yuan et al., 2012; Fulda et al., 2013b; Fulda et al., 2013a). In our speciation calculations, we have not accounted for the formation of these Cu(I)-thiol complexes, and dissolved Cu is assumed to be in Cu(II) form.

2.6 Kinetic model

A kinetic model was developed to quantify the effect of Cu on denitrification. Michaelis-Menten expressions were used to describe the evolution of NO_3^-, NO_2^-, N_2O, and N_2 during denitrification (Eq 1-4).

$$\frac{d[NO_3^-]}{dt} = -V_{max}\frac{[C_{NO_3^-}]}{K_{NO_3^-} + [C_{NO_3^-}]} \quad (1)$$

$$\frac{d[NO_2^-]}{dt} = V_{max}\left(\frac{[C_{NO_3^-}]}{K_{NO_3^-} + [C_{NO_3^-}]} - \frac{[C_{NO_2^-}]}{K_{NO_2^-} + [C_{NO_2^-}]}\right) - k_{ab}[C_{NO_2^-}] \quad (2)$$

$$\frac{d[N_2O]}{dt} = V_{max}\left(\frac{[C_{NO_2^-}]}{K_{NO_2^-} + [C_{NO_2^-}]} - \frac{[C_{N_2O}]}{K_{N_2O} + [C_{N_2O}]}\right) \quad (3)$$

$$\frac{d[N_2]}{dt} = V_{max}\left(\frac{[C_{N_2O}]}{K_{N_2O} + [C_{N_2O}]}\right) + k_{ab}[C_{NO_2^-}] \quad (4)$$

Here, V_{max} denotes the maximum reaction rate under unlimited substrate supply (mmol-N L^{-1} day^{-1}), C_y are the concentrations of N-containing species (mmol-N L^{-1}), and K_y values are Michaelis-Menten parameters (mmol-N L^{-1}) describing the substrate concentration at which the reaction rate is half V_{max} (Bowman and Focht, 1974; Kremen et al., 2005). For model development, the concentration of N_2 was calculated from the mass balance on nitrogen species. As discussed earlier, abiotic nitrite reduction to N_2 by inorganic electron donors, such as inorganic sulfur compounds (S^o, S^{2-}, $S_2O_3^{2-}$), pyrite (FeS_2), thiocyanate (SCN^-), and ferrous ion (Fe^{2+}), is a pathway in N-cycling (Zhu and Getting, 2012; Zhu-Barker et al., 2015; Di Capua et al., 2019; Otte et al., 2019). Therefore an additional reaction, accounting for the abiotic reduction of NO_2^- to N_2, was included in the model. A pseudo first-order reaction was used to define the abiotic reduction of NO_2^- in the system (incorporated in Eq 2 and 4), where k_{ab} (day^{-1}) is the pseudo first-order rate constant assuming that the reductants are in excess (Matocha et al., 2012; Chen et al., 2020), and $C_{NO_2^-}$ is the concentration of NO_2^- in the dissolved phase. Using the ODE45 function in MATLAB R2018a (Shampine et al., 2003; Anyigor and Afiukwa, 2013), the unknown parameters were calculated. The value of V_{max} was determined using Eq 1 and data on the change in nitrate concentration with time, and then the

value was fixed to determine the rate parameters defined in Eq 2-4. A constant value of V_{max} can be employed when organic carbon is present in excess of NO_3^- (Kremen et al., 2005). The total organic carbon present in the systems studied far exceeded the amount of NO_3^- added (Section S2 in SM). In separate optimations in which we allowed the values of V_{max} to be different in equations 1-4, the values were all in the narrow range of range 0.25 – 0.5 mmol-N L^{-1} day^{-1}.

3. Results

3.1 Characterization of soils and sediments

Both the surface water samples, and the soils and sediments were characterized to determine their total carbon, sulfur, metals, and nutrient concentrations. The detailed results are presented in our recent study focused on trace metal micronutrient speciation in wetland soils and stream sediments (Yan et al., 2021). The surface water in the marsh wetlands (Marsh 1) and stream sediments (Stream 1 and Stream 2) had pH values ranging from 7.5-8.1, and they contained high concentrations of calcium, magnesium, and sulfate. However, the riparian wetland surface water samples (Riparian 1 and Riparian 2) were at pH 5.5-6.0 with substantially lower concentrations of major elements.

The mineralogy at all of the studied sites is dominated by quartz, with variations in minor phases (Yan et al., 2021). The total organic carbon content of aquatic systems varies with location: the marsh wetland site (Marsh 1) contained the highest carbon content (9.0%), whereas Stream 2 exhibited the lowest carbon content (0.5%) (Table S2). The sulfur content was low at all sites (below 0.24%), following the trend Marsh 1 > Riparian 2 ≈ Stream 1 > Riparian 1 ≈ Stream 2. The concentrations of Cu were well below the crustal abundance (428 ± 61 nmol/g) (Rudnick and Gao, 2003) at all the studied sites. The marsh wetland soil (Marsh 1) and Riparian 2 location in the riparian wetlands contained higher concentrations of solid-phase Cu than the other locations. The total Fe concentration in the solid phases was similar at all the sites (200 to 460 µmol/g), except for Riparian 1, which contained an order of magnitude less Fe than the other soils/sediments. The concentration of Mn was two to three orders less than the Fe content, with the highest values observed in stream sediments. Extractable ammonium in soils/sediments was greater than extractable

294 NO_3^- and NO_2^- at all the locations, which may indicate denitrification and/or ammonium retention via cation
295 exchange (Table S2).

296 **3.2 Evolution of nitrogen species concentrations during incubation**

297 The controls and the low-Cu amended sets showed similar NO_3^- reduction profiles in all the systems
298 studied (Figure 2). However, a small delay in NO_3^- reduction after Cu addition was observed at high Cu
299 loading in Riparian 1, Riparian 2, and Stream 2 incubation experiments (Figure 2a, 2e, and 2m). In Riparian
300 1 and Stream 2 experiments, complete reduction of NO_3^- did not occur, even after 27 days and 20 days of
301 incubation, respectively.

302 The presence of detectable NO_2^- was transient and showed a brief appearance followed by a rapid
303 decline in concentration in Riparian 2, Stream 1, and Marsh 1 incubations. In Riparian 1 soils, the dissolved
304 NO_2^- concentrations were below the detection limit (0.0005 mmol-N L^{-1}) throughout the experiment,
305 suggesting rapid conversion of NO_2^- in these soils (Figure 2b). In the case of Riparian 2 and Stream 2
306 systems, Cu addition affected NO_2^- formation/reduction because more NO_2^- was detected in controls as
307 compared to Cu-amended sets.

308 For all the systems studied, less N_2O accumulated in the sets amended with Cu. We did not observe
309 persistent accumulation of N_2O in the case of Riparian 1 soils (Figure 2c), however, the maximum
310 concentration of N_2O (control: 0.040 mmol-N L^{-1} at 14 days, low-Cu: 0.032 mmol-N L^{-1} at 10 days, and
311 high-Cu: 0.021 mmol-N L^{-1} at 12 days) decreased as the dissolved Cu concentration increased. For Riparian
312 1 controls and low-Cu amended microcosms, N_2O started to accumulate after 3 days of incubation, whereas
313 in high-Cu amended sets, N_2O accumulation was only observed after 6 days of incubation. The complete
314 reduction of N_2O to N_2 was fast in low-Cu amended Riparian 1 sets; we did not observe N_2O after 14 days
315 in low-Cu added sets, whereas it took 29 and 23 days to completely reduce N_2O in high-Cu added and
316 control sets, respectively. In the Riparian 2 control, N_2O accumulated in the headspace and persisted until
317 the end of the experiment at 30 days, whereas the N_2O concentration first increased and then decreased
318 after 10 days and 16 days in Riparian 2 sets amended with low Cu and high Cu, respectively (Figure 2g).

For Riparian 2, relative to controls, the maximum N_2O concentration decreased by 38.6% in low Cu-added sets and by 70.1% in high Cu-added sets. In the case of the stream sediments, Stream 1 showed a significant effect of Cu addition on N_2O reduction; with respect to controls, the peak N_2O concentration decreased by 2.6 times and 7.8 times in sets with low and high Cu loading, respectively (Figure 2k). In Stream 2 and Marsh 1 systems, we were able to measure detectable N_2O in the headspace of only the controls; in the Cu-amended sets, any N_2O generated was rapidly reduced before the N_2O reached detectable levels (Figure 2n and 2r).

The concentration of dissolved ammonium (NH_4^+) remained relatively constant throughout the experiment for all the treatments (control, low loading, and high loading) in the systems studied (Figure 2). Dissolved NH_4^+ was highest in Marsh 1, at 1.039 ± 0.048 mmol-N/L. Riparian 2 and Riparian 1, contained 0.130 ± 0.004 mmol-N/L and 0.033 ± 0.004 mmol-N/L NH_4^+, respectively. The dissolved NH_4^+ concentrations in stream sediments averaged 0.053 ± 0.005 mmol-N/L and 0.172 ± 0.019 mmol-N/L in the Stream 1 and Stream 2 samples, respectively.

3.3 Variation in dissolved metal (Cu, Fe, and Mn) concentration

Dissolved Cu, Fe, and Mn were monitored throughout the incubation experiments (Figure 3). The dissolved Cu concentrations in the unamended control microcosms followed the trend Marsh 1 > Riparian 2 > Riparian 1 > Stream 2 > Stream 1. The dissolved Cu concentration remained relatively constant throughout the experiment for Riparian 2, Stream 2, and Stream 1 experiments. However, a decrease in Cu concentration was observed in all Riparian 1 sets, and controls and low-Cu amended Marsh 1 sets in the initial days of incubation (Figure 3d and 3m).

A decrease in dissolved Fe concentration was observed during the experiment for the riparian wetland soils (Riparian 1 and Riparian 2) and stream sediments (Stream 1 and Stream 2), whereas, in marsh wetland soil (Marsh 1), dissolved Fe concentration did not fluctuate during the 8 days of incubation (Figure 3). In the Riparian 1 and Riparian 2 experiments, the dissolved Mn concentration remained constant and was similar for all treatments (control, low and high Cu-loadings). However, in Stream 1 and Marsh 1, we

observed a decrease in the concentration of Mn until 7 days and 4 days, respectively and then it remained constant (Figure 3i and 3o). Mn concentrations in Stream 2 experiments amended with high Cu were greater than the concentrations in controls and low Cu-loading experiments (Figure 3l).

3.4 Effect of Cu addition on denitrification rate

The effect of Cu on denitrification was quantified with the help of the kinetic model. We obtained Michaelis-Menten parameters (Table 2) and the abiotic rate constant for the set of differential equations defined earlier (Eq 1-4). Here, $K_{NO_3^-}$, $K_{NO_2^-}$, and K_{N_2O} values reflect the ability of the microbial community present in the soils and sediments to reduce NO_3^- to NO_2^-, NO_2^- to NO, and N_2O to N_2, respectively under the conditions studied. NO is rapidly transformed to N_2O, hence the conversion of NO to N_2O was assumed to not be rate-limiting. The rate constant for abiotic reduction of NO_2^- to N_2 by inorganic donors in the system is defined by k_{ab}, and inclusion of this reaction helped us reproduce the major features of all the experiments (Figure 4). The abiotic reduction of NO_2^- to N_2O is also a possible pathway, but the incorporation of this reaction into the kinetic model did not improve the fit to experimental data. Michaelis-Menten parameters have an inverse relationship with rates, unlike rate constants; the smaller the value of K_y, the faster the forward reaction; whereas the greater the value of k_{ab}, the faster the rate of abiotic nitrite reduction. The model was able to describe the major features for nitrogen species reduction at all the sites except for Marsh 1. For the Marsh 1 site, we observed a lag in NO_3^- reduction in all the incubation experiments. Our model does not account for the acclimatization time of microorganisms after NO_3^- an addition which could have caused poor fitting of data from the Marsh 1 experiments.

The modeled $K_{NO_3^-}$ values show that NO_3^- reduction is fastest in Stream 1 sediments followed by Marsh 1, Riparian 2, Riparian 1, and Stream 2. The parameter $K_{NO_3^-}$ was similar for control and low Cu-loading in all the systems studied. However, the modeled value increased (Table 2) in high Cu-loading sets initiated with Riparian 1, Riparian 2, and Stream 2 sediments, indicating that the reduction of NO_3^- to NO_2^- is slower in these sets amended with a high concentration of Cu.

Cu addition decreased NO_2^- accumulation in Riparian 2 and Stream 2 samples. The value of $K_{NO_2^-}$ was less in Cu-amended Riparian 2 experiments (control: 0.68 mmol-N L^{-1}; low Cu: 0.22 mmol-N L^{-1}; and high Cu: 0.33 mmol-N L^{-1}), which signified that Cu enhanced the rate of NO_2^- reduction in Riparian 2 soils. Similarly, in Stream 2 sediments, the modeled $K_{NO_2^-}$ values show a substantial decrease in Cu-amended sets (control: 0.0.079 mmol-N L^{-1}; low Cu: 0.0067 mmol-N L^{-1}; and high Cu: 0.0035 mmol-N L^{-1}).

The rate of N_2O to N_2 conversion, as indicated by the K_{N_2O} parameter, increased upon Cu addition in the Riparian 1, Riparian 2, Stream 1, and Stream 2 locations. In the marsh wetland soil, K_{N_2O} remained relatively constant in the control and Cu-amended experiments. The effect of Cu addition on N_2O reduction was greatest in the Riparian 1 and Riparian 2 soils; in Riparian 2 soils, the value of K_{N_2O} decreased from 11000 mmol-N L^{-1} in unamended control experiments to 0.48 mmol-N L^{-1} and 0.21 mmol-N L^{-1} in low-Cu loading and high-Cu loading experiments, respectively. Similarly, in Riparian 1 soils, Cu addition increased the N_2O conversion significantly; K_{N_2O} values decreased from 6900 mmol-N L^{-1} to 24 mmol-N L^{-1} and 3.5 mmol-N L^{-1} at low and high Cu loadings, respectively.

The rate of abiotic NO_2^- to N_2 reduction was greater in Riparian 1 and Riparian 2 wetland soils than in the other three systems; all microcosms incubated with Stream 2 sediments and Marsh 1 soils showed negligible k_{ab} values. NO_2^- was not detected in any Riparian 1 incubation experiments (Figure 2b); the abiotic rate constant for NO_2^- to N_2 reduction is high in Riparian 1 soils, which could have prevented NO_2^- accumulation in these soil incubations. The values of k_{ab} were similar for all the different incubation studies (controls, low-Cu, and high-Cu loading) of a location, signifying that this step is not affected by the presence of Cu.

3.5 Labile concentration of Cu in soil/sediment incubations

To understand Cu bioavailability as a nutrient and as a toxic element, we estimated the speciation of dissolved Cu using Visual MINTEQ 3.1 and the NICA-Donnan model at the studied experimental conditions and in the presence of dissolved organic carbon (Figure 5). The calculations predict that DOC substantially decreased the lability of Cu in the systems studied. Here, the labile Cu concentration is defined

as the sum of Cu^{2+}, $Cu(OH)^{+}$, and $Cu(OH)_{2(aq)}$. In riparian wetland controls, Riparian 1 and Riparian 2, in the studied pH range (5-6), Cu is predominantly present as Cu-organic matter complexes (Figure 6), and the labile Cu concentration (Table S4), is < 3 nM. Similarly, in Stream 1 controls, the total labile Cu concentration is < 1 nM in the experimental pH range (7.6-9.0). Due to a lower concentration of DOC in Stream 2 (Figure 5), ~80% of dissolved Cu is present as labile Cu in Stream 2 controls. High DOC in Marsh 1 samples complexed ~84% of dissolved Cu(II), and only 7.6 nM remained as labile concentration in the fluid of controls. In all the Cu-amended experiments, the lability of Cu was greater than the optimum concentration (~3 nM) determined to complete N_2O to N_2 conversion in pure culture studies and lake systems (Iwasaki et al., 1980; Granger and Ward, 2003; Twining et al., 2007). Additionally, in high-Cu amended experiments, labile Cu in Riparian 1, Riparian 2, and Stream 2 was substantially higher (> 350 nM), which could inhibit biological denitrification due to toxic effect (Allen and Hansen, 1996; Kozelka and Bruland, 1998; Huang and Wang, 2003).

4. Discussion

4.1 Effect of Cu addition on nitrogen cycling

This study found that high dissolved Cu concentrations inhibited NO_3^- reduction to NO_2^- in the riparian wetland soils (Riparian 1 and Riparian 2) and from the Stream 2 sediments. This observation is in line with previous results: higher concentrations of Cu can inhibit denitrification by causing a shift in the community composition of denitrifiers (Magalhaes et al., 2007; Wang et al., 2018; Zhao et al., 2020). A recent study that focused on evaluating the toxic effects of copper oxide (CuO) nanoparticles on denitrification in soils observed that the Cu ions (Cu^{2+}) released upon nanoparticle application can decrease nitrate reductase (Nar) activity by 21.1- 42.1%, causing an 11-times decrease in NO_3^- reduction (Zhao et al., 2020). Elevated Cu^{2+} concentrations (> 500 µg g^{-1} in solid-phase and ~0.95 mg L^{-1} in dissolved form) can decrease biological denitrification by inhibiting extracellular or intracellular enzymes (Fu and Tabatabai, 1989; Sakadevan et al., 1999; Ochoa-Herrera et al., 2011). At high Cu loadings in the above-mentioned locations (Riparian 1, Riparian 2, and Stream 2), the labile Cu concentrations estimated using the NICA-Donnan model were

418 higher (> 350 nM) than in Stream 1 (28 nM) and Marsh 1 (150 nM) locations (Table S4), and the higher
419 concentratons could have inhibited NO_3^- reduction during the incubation experiments.

420 Incomplete reduction of NO_3^- was observed in incubation experiments using Riparian 1 soils and
421 Stream 2 sediments even when Cu was not added and had low labile concentrations. This suggests that
422 denitrification was limited by the low total organic carbon content at these sites (Table S2). While the total
423 organic carbon present in the soils/sediments exceeded the amount stoichiometrically required for complete
424 reduction of NO_3^- (Section S2 in SM), not all of the organic carbon will be available to denitrifying
425 microorganisms (Schmidt et al., 2017). The biodegradability of the organic matter depends upon molecular
426 characteristics of the organic matter; carbohydrates, proteins, and organic acids are easily degradable,
427 whereas, aromatic and hydrophobic organic entities are recalcitrant to microbial activity (Marschner and
428 Kalbitz, 2003). The low degradability of organic matter is probably limiting NO_3^- reduction in Riparian 1
429 and Stream 2 sites.

430 The dissolved Cu concentration in the Riparian 2 control (41 ± 9 nM) was higher than the optimum
431 concentration required for N_2O to N_2 conversion in pure culture studies (3 to 10 nM) (Granger and Ward,
432 2003; Twining et al., 2007; Glass and Orphan, 2012). However, N_2O accumulation was observed at the
433 Riparian 2 site, suggesting that the dissolved Cu may not have been completely bioavailable to the
434 microorganisms that convert N_2O to N_2. The high DOC (47 mg C/L) at Riparian 2 (Figure 5) indicated the
435 presence of soluble organic ligands. These ligands may form soluble complexes with Cu, thus decreasing
436 Cu availability (Du Laing et al., 2009; Zhang et al., 2014). The free Cu^{2+} and the Cu(II)-hydroxo complexes
437 concentrations control the bioavailability of Cu rather than the total dissolved concentration (Black et al.,
438 2011; Bourgeault et al., 2013). The labile Cu concentration in Riparian 2 control experiments, shown as
439 the sum of Cu^{2+}, $Cu(OH)^+$, and $Cu(OH)_{2(aq)}$ (Table S4), is ~ 1.4 nM which is less than the optimum Cu
440 concentration (> 3 nM) (Granger and Ward, 2003; Glass and Orphan, 2012) required for conversion of N_2O
441 to N_2 in pure culture studies. Thus, the low lability of Cu in Riparian 2 control sets could have caused
442 persistent N_2O accumulation in the headspace.

In Riparian 1 soils, both the background dissolved Cu concentration (29.3 nM) and the solid-phase-associated Cu (48.3 nmol/g) were less than the Cu concentration in Riparian 2 soils (dissolved: 41 nM; solid-phase: 262.3 nmol/g), but N_2O did not accumulate persistently in the headspace of Riparian 1 soils. This observation suggests that bioavailable Cu for N_2O to N_2 conversion is more abundant in Riparian 1 soils. Riparian 1 soils have less dissolved organic carbon (23 mg C/L) than Riparian 2 soils, and thus are less able to decrease the bioavailability of Cu by forming soluble complexes of organic matter with Cu. The speciation results corroborated the hypothesis because in the pH range studied, the dissolved labile Cu in Riparian 1 controls (2.8 ± 0.9 nM) was greater than Riparian 2 controls (1.4 ± 0.8 nM). Prior study on a lake system indicated that the presence of 3 nM dissolved Cu decreased N_2O accumulation during denitrification relative to systems containing no Cu (Twining et al., 2007). Although the rate of N_2O to N_2 conversion was slow in Riparian 1 controls as compared to Cu-amended sets (Table 2), the labile-Cu concentration closer to ~ 3 nM prevented persistent N_2O accumulation in the headspace.

The concentration of accumulated N_2O in the headspace of Stream 1 controls was greater than the Stream 2 controls. Both stream sediment sites contained low concentrations of dissolved Cu in the control sets (3.1 ± 1 nM at Stream 1, and 6.2 ± 1.9 nM at Stream 2), however, substantial N_2O accumulation was only observed at Stream 1 location. This finding suggests that the low Cu concentrations of ~ 6 nM were sufficient to enable the N_2O to N_2 conversion in Stream 2 sediments. The dissolved organic carbon concentration is lower at the Stream 2 location (2.1 mg C/L, Figure 5) which indicated that the fraction of dissolved Cu that is labile (i.e., not complexed with organic ligands) would be higher for Stream 2 (labile Cu in Stream 1: 0.55 nM and Steam 2: 4.8 nM). Thus, the presence of un-complexed Cu(II) at a concentration of ~ 4.8 nM enabled N_2O to N_2 conversion in Stream 2 controls.

N_2O was not detected in the headspace of Marsh 1 Cu-amended microcosms, however, we observed accumulation of N_2O in unamended control experiments in the initial days of incubation (max N_2O: 0.064 mmol-N/L). This observation suggests that the rate of N_2O to N_2 conversion was promoted by Cu amendment in Marsh 1 site (Figure 2s). The dissolved Cu concentration in the control samples was 48 nM, which is higher than the optimal values (3 to 20 nM) for N_2O transformation in pure culture studies (Granger

and Ward, 2003; Glass and Orphan, 2012). The dissolved organic carbon (32 mg C/L) at the site is calculated to have decreased the bioavailability of Cu substantially (labile Cu in controls: 7.6 ± 5 nM) in the pH range studied, thus resulting in the transient N_2O accumulation in the headspace of the unamended controls.

4.2 Ammonium release during the incubations

In all the locations studied, a substantial amount of NH_4^+ was detected in the dissolved phase and remained constant throughout the experiment (Figure 2). Exchangeable NH_4^+ can be released from the solid phase to the fluid because of changes in the water-to-solid ratio, pH, and ionic strength. Alternatively, the NH_4^+ can result from the microbially-mediated dissimilatory nitration reduction to ammonium (DNRA) (Wang et al., 2008; Robertson and Thamdrup, 2017; Zhu et al., 2019; Liu et al., 2020; Wang et al., 2020). The ammonium was released into the fluid phase even before the onset of NO_3^- reduction (Figure 2), and the concentration of NH_4^+ remained constant throughout the experiment. This observation indicated that most of the released NH_4^+ was due to exchange from the soils/sediments and not due to biological nitrate reduction. Additionally, the mass balance of extractable ammonium in soils/sediments indicates that the soils/sediments have the capacity to release the amounts of NH_4^+ observed in the fluid (Riparian 1: 0.05 mmol-N L^{-1}, Riparian 2: 0.14 mmol-N L^{-1}, Stream 1: 0.15 mmol-N L^{-1}, Stream 2: 0.14 mmol-N L^{-1}, and Marsh 1: 1.04 mmol-N L^{-1}).

4.3 Relationship between pH, dissolved metal content, and denitrification

During the initial 2-3 days of incubation, the pH increased from 5.0 to ~ 6.5 for Riparian 1 and Riparian 2 soils, from 7.6 to ~ 8.9 for Stream 1 and Stream 2 sediments, and from 7.0 to ~ 8.2 for Marsh 1 soils, and then remained relatively constant. The increase in pH values can be attributed to NO_3^- and NO_2^- reduction during denitrification. Previous study on riparian soils indicated that the pH increased from 5 to 7 and 5 to 9 in unbuffered NO_3^- reduction experiments with low (111 μmol N g^{-1}) and high (500 μmol N g^{-1}) nitrogen loadings, respectively (Clement et al., 2005). In contrast, pH variation was limited (± 0.5) when

denitrification occurred in carbonate-buffered lowland soils from Northern Italy (Castaldelli et al., 2019). Our previous study on the studied natural aquatic systems indicated that these soils and sediments lacked carbonate minerals (Yan et al., 2021); hence, the buffering capacity of the soils/sediments was likely inadequate to prevent the increase in pH upon NO_3^- and NO_2^- reduction.

The dissolved concentrations of Cu, Fe, and Mn were indirectly affected by nitrogen cycling in the incubation experiments. The decrease in Cu concentrations in Riparian 1 systems and controls and low-Cu amended sets of Marsh 1 soils (Figure 3a, 3d and 3m) likely resulted from an increase in Cu adsorption with increasing pH. We also observed that substantial amounts of Fe and Mn were released into the water in all of the incubation experiments after 24 h of incubation, indicating the reductive dissolution of Fe/Mn oxyhydroxides under anaerobic conditions (Zhang et al., 2014). The released Fe decreased over time in the Riparian 1, Riparian 2, Stream 1, and Stream 2 sites. Under the conditions studied, dissolved Fe predominantly exists as Fe(II); the extent of Fe(II) sorption on clays, silica, and metal-oxide phases increases with an increase in pH (Schultz and Grundl, 2004; Nano and Strathmann, 2006; Zhu and Elzinga, 2014). Additionally, Fe(II) may serve as an electron donor for the abiotic reduction of NO_3^- and NO_2^- to form N_2 in soils and sediments (Eq 5-6) (Burgin and Hamilton, 2007; Klueglein et al., 2014; Robertson and Thamdrup, 2017; Liu et al., 2019; Otte et al., 2019; Rahman et al., 2019; Robinson et al., 2021).

$$NO_3^- + 5Fe^{2+} + 12H_2O \rightarrow \frac{1}{2}N_{2(g)} + 5Fe(OH)_3 + 9H^+ \quad (5)$$

$$NO_2^- + 3Fe^{2+} + 7H_2O \rightarrow \frac{1}{2}N_{2(g)} + 3Fe(OH)_3 + 5H^+ \quad (6)$$

Although the abiotic reduction of NO_3^- to N_2 in the presence of Fe(II) is thermodynamically feasible, studies indicate that NO_3^- can only be directly reduced by Fe(II) in the presence of mixed-valence Fe-bearing solids (green-rusts), or a catalyst, such as Cu(II), Sn(II), and Ag(I) (Ottley et al., 1997; Davidson et al., 2003). Fe(II) adsorbed to iron-oxide surfaces is a stronger reducing agent than Fe(II) in dissolved form (Stumm and Sulzberger, 1992; Davidson et al., 2003), hence adsorbed Fe(II) might promote NO_3^- reduction in the studied systems. Additionally, biological oxidation of structural Fe(II) in clay minerals, such as illite and nontronite, can be coupled with reduction of NO_3^- to N_2 (Zhao et al., 2013; Zhao et al., 2017). In our

incubation studies, the dissolved Fe concentration decreased until 27, 18, and 6 days in Riparian 1, Riparian 2, and Stream 1 systems, respectively and then remained almost constant through the end of the experiments. Decreases in Fe concentration were only observed until the NO_3^-/NO_2^- were completely consumed in these systems indicating that Fe(II) oxidation to Fe(III) oxides/hydroxides is coupled abiotically or biotically to NO_3^-/NO_2^- reduction at Riparian 1, Riparian 2, and Stream 1 sites. Mass balance calculations indicated that NO_3^- concentrations were sufficient to allow for consumption of Fe(II) in Riparian 1, Riparian 2, and Stream 1 systems to react with Fe(II) (Section S3 in SM). The values of k_{ab} relative to $K_{NO_2^-}$ were high in Riparian 1, Riparian 2, and Stream 1 systems, suggesting that the reaction involving abiotic NO_2^- reduction is substantial in these systems. On the other hand, the decrease in the Fe(II) concentration in Stream 2 experiments aligned with the pH increase during the initial 2-3 days of incubation, so the decrease in Fe concentration could also be due to increased adsorption at higher pH.

The addition of Cu affected Mn concentrations in Stream 2 experiments; the release of Mn was greater in sets amended with high Cu (Figure 3l). In stream 2 incubation experiments with high Cu loading, 250 µM Cu was added and only 0.60 µM remained in the dissolved phase after 24 h equilibration; the competitive adsorption of Cu(II) onto active sites of mineral-phases could have mobilized Mn(II) (~ 40 µM in this case) to the water. Prior studies have also observed the release of Mn(II) in the presence of Cu due to competitive adsorption (Kurdi and Donner, 1983; Traina and Doner, 1985). In Stream 1 and Marsh 1 studies, the concentration of dissolved Mn decreased with time (Figure 3i and 3o). Mn adsorption has been found to increase with pH on clay minerals, iron oxides/hydroxides and aluminum oxides. In reducing NO_3^-, Mn^{2+} can also serve as an electron donor (Eq 7) to autotrophic denitrifiers belonging to the genera *Acinetobacter* and *Pseudomonas* (Su et al., 2015; Su et al., 2016).

$$Mn^{2+} + 0.4NO_3^- + 0.8H_2O \rightarrow MnO_2 + 0.2N_2 + 1.6H^+ \quad (7)$$

Thus, the decrease in the concentration of Mn observed in Stream 1 and Marsh 1 samples can result from increased adsorption caused by a shift in pH or from Mn consumption by autotrophic denitrifiers.

4.4 Comparison of nitrogen cycling with materials from different systems

The studied aquatic systems, even different locations of the same site, showed varied trends in the reduction of nitrogen species in the incubation experiments. The total dissolved Cu concentrations in both locations of EFPC stream sediments (Stream 1 and Steam 2) were very low (3-10 nM), but transient N_2O accumulation only occurred in their unamended controls, whereas TB riparian wetland soils (Riparian 1 and Riparian 2) showed substantial N_2O accumulation despite having much higher dissolved background Cu concentrations of 30-50 nM. This disparity suggests that the speciation of Cu, and hence its bioavailability, plays a more important role than the total Cu content in controlling N_2O to N_2 conversion in the studied environmental systems.

Even after Cu addition, the accumulated concentrations of N_2O in the riparian wetland samples were higher than in the other locations. One possible explanation is that the riparian wetland incubation experiments were conducted at pH 5, whereas the incubations for marsh wetland soils (Marsh 1) and stream sediments (Stream 1 and Stream 2) were performed at neutral pH conditions. Acidic soils decrease the activity of the nitrous oxide reductase enzyme, leading to N_2O accumulation (Knowles, 1982; Simek and Cooper, 2002; Pan et al., 2012; Carreira et al., 2020). Optimal N_2O reduction has been observed in the pH range of 7.5-8.0; previous studies have observed substantial N_2O accumulation in the pH range of 6.0-6.5 (Pan et al., 2012; Carreira et al., 2020). Although the pH in the riparian wetland soils increased to ~ 6.5 in the first two days of incubation, i.e., before the onset of N_2O accumulation, it was in the range where a decrease in the activity of nitrous reductase enzyme has been observed (Pan et al., 2012; Carreira et al., 2020). Thus, Riparian 1 and Riparian 2 wetland soils could be a significant source of N_2O, not only because the bioavailable Cu is limited but also because they are acidic.

5. Geochemical significance and implications

Most pristine natural aquatic systems contain low solid-phase Cu, and hence they may have low availability of Cu for microbial denitrification. The limited set of studies on natural aquatic systems containing Cu at concentrations less than or equal to crustal abundances (441±63 nmol g^{-1}) support our

major finding that increased Cu concentrations can increase the extent of conversion of N_2O to N_2. At 26 μM dissolved Cu, Giannopoulos et al. (2020) concluded that greater availability of Cu led to less N_2O accumulation and higher abundance of Cu-dependent enzymes in wetland soils. A study on agricultural soils indicated that the application of organic fertilizer modified with 130 mM $CuSO_4$ decreased N_2O emissions substantially (Shen et al., 2020). However, these above-mentioned studies evaluated Cu concentrations that are relatively higher than the optimum concentrations (3-10 nM) required for N_2O to N_2 transformation in pure culture studies. The concentrations of dissolved Cu in natural environments are typically low (< 200 nM), and the presence of inorganic/organic ligands can further decrease the bioavailability of Cu causing incomplete denitrification with N_2O accumulation. Our results indicated that without Cu amendment, substantial N_2O accumulation can take place in soils and sediments.

The selected sites represent different aquatic systems in geologically-distinct regions and contain low solid-phase and dissolved Cu (solid-phase: 45-280 nmol g^{-1} and dissolved: 3-48 nM). Despite the differences in mineralogy, elemental composition, and aqueous-phase characteristics, the presence of dissolved Cu at trace levels (10-500 nM) decreased N_2O accumulation in all the sites. The response of riparian wetland soils (Riparian 1 and Riparian 2) to Cu addition was less pronounced than that of other studied sites, which highlights that that the systems with acidic conditions like Riparian 1 and 2 can be substantial contributors of N_2O emissions even in the abundance of Cu.

Our study provides greater insight into the importance of Cu speciation on cycling of nitrogen species in environmental systems The effect of Cu on N_2O accumulation was more closely associated with estimated labile-Cu concentrations than with total dissolved Cu concentrations. Dissolved Cu in the porewater of soils and sediments was substantially lower than the total solid-phase associated concentration, and its lability is lowered by its interactions with dissolved organic matter (Bourgeault et al., 2013; Zhang et al., 2014).

For systems with Cu limitations of complete denitrification, our results indicate that the addition of minor amounts of Cu can increase the rate of N_2O conversion in natural aquatic systems Natural soils have been recognized as an important source of N_2O to the atmosphere and are estimated to release up to 5.6 Tg

593 N_2O-N yr^{-1} (Tian et al., 2020). Current ecosystem models, such as DLEM, incorporate multiple
594 environmental factors, including moisture content, temperature, nitrate and dissolved organic carbon
595 concentration, and pH, in the estimation of N_2O emissions from terrestrial systems (Tian et al., 2015). These
596 models do not account for the effect of trace metal micronutrient availability (Cu, Ni, Zn, Co, and Mo) on
597 biogeochemical processes responsible for the release of greenhouse gas emissions. The inclusion of Cu as
598 an additional parameter can help improve the accuracy of existing ecosystem models to predict N_2O
599 emissions from soils and sediments. Addition of trace amounts of Cu to natural aquatic systems could
600 potentially decrease N_2O release to the atmosphere. Changes in Cu speciation in wetlands and stream
601 sediments associated with hydrologic variation could also influence net N_2O emissions.

602 ## 6. Conclusions

603 Through a combination of incubation experiments and a kinetic model we determined the effect of dissolved
604 Cu at trace levels (10-500 nM) on the rate of N_2O reduction. Only the systems containing estimated labile
605 Cu < 10 nM had substantial N_2O accumulation. Even with a small increase in dissolved Cu concentration,
606 as observed in low-Cu-loaded incubation experiments, the rate of N_2O to N_2 conversion was significantly
607 enhanced. The contribution of the abiotic reduction of NO_2^- to N_2 by Fe(II) was significant at Riparian 1,
608 Riparian 2, and Stream 1 locations. Riparian wetland soils showed higher N_2O accumulation than the other
609 sites studied, indicating that the acidic pH conditions can enhance N_2O emissions from natural
610 environments. The sites containing high concentrations of DOC (Riparian 1, Riparian 2, and Marsh 1) had
611 less concentrations of dissolved Cu that were labile and showed greater N_2O accumulation. Our results
612 indicate that including Cu bioavailability in ecosystem models could improve the accuracy of estimates of
613 N_2O emissions from natural landscapes.

614 ## Acknowledgements

615 This project was supported by the U.S. Department of Energy, Office of Science, Office of Biological and
616 Environmental Research, Subsurface Biogeochemical Research program through award no. DE-
617 SC0019422 to Washington University. We acknowledge our collaborators, Pamela Weisenhorn, Edward J.

O'Loughlin, and Kenneth M. Kemner at Argonne National Laboratory, Grace E. Schwartz and Scott C. Brooks at Oak Ridge National Laboratory, and Daniel I. Kaplan at Savannah River National Laboratory, who helped us in collecting samples from the selected aquatic systems. We thank Jinshu Yan, a doctoral student in the Department of Earth and Planetary Sciences for characterizing the soils/sediments used for the incubation experiments. ICP-MS measurements were performed in the Nano Research Facility (NRF) at Washington University in St. Louis. We also thank the McDonnell International Scholars Academy for the fellowship that is supporting Neha Sharma in her graduate program. We also thank James Ballard for assisting us in improving the quality of writing in this manuscript.

Appendix A. Supplementary Material

The supplementary material includes information on the recipe of the simulated water used for Cu uptake and incubation experiments, concentrations of solid-phase associated metals and nutrients, methodology and parameters used for estimating Cu speciation in the presence of dissolved organic carbon, the concentration of estimated labile Cu using NICA-Donnan model, and the calculations showing organic matter and Fe(II) requirements for nitrate reduction during the incubation experiments.

Research Data

Data associated with this article can be accessed at https://data.mendeley.com//datasets/t359pdpcxy/1.

References

Allen H. E. and Hansen D. J. (1996) The importance of trace metal speciation to water quality criteria. *Water Environ. Res.* **68**, 42–54.

Anyigor C. and Afiukwa J. (2013) Application of matlab ordinary differential equation function solver (ode45) in modelling and simulation of batch reaction kinetics. *Am. J. Sci. Ind. Res.* **4**, 285–287.

Baeseman J. L., Smith R. L. and Silverstein J. (2006) Denitrification potential in stream sediments impacted by acid mine drainage: Effects of pH, various electron donors, and iron. *Microb. Ecol.* **51**, 232–241.

Benedetti M. F., Milne C. J., Kinniburgh D. G., Van Riemsdijk W. H. and Koopal L. K. (1995) Metal ion binding to humic substances: Application of the non-ideal competitive adsorption model. *Environ. Sci. Technol.* **29**, 446–457.

Benedetti M. F., Van Riemsdijk W. H. and Koopal L. K. (1996) Humic substances considered as a heterogeneous Donnan gel phase. *Environ. Sci. Technol.* **30**, 1805–1813.

Bertero M. G., Rothery R. A., Palak M., Hou C., Lim D., Blasco F., Weiner J. H. and Strynadka N. C. J. (2003) Insights into the respiratory electron transfer pathway from the structure of nitrate reductase A. *Nat. Struct. Biol.* **10**, 681–687.

Black A., Hsu P. C. L., Hamonts K. E., Clough T. J. and Condron L. M. (2016) Influence of copper on expression of nirS, norB and nosZ and the transcription and activity of NIR, NOR and N_2OR in the denitrifying soil bacteria Pseudomonas stutzeri. *Microb. Biotechnol.* **9**, 381–388.

Black A., McLaren R. G., Reichman S. M., Speir T. W. and Condron L. M. (2011) Evaluation of soil metal bioavailability estimates using two plant species (L. perenne and T. aestivum) grown in a range of agricultural soils treated with biosolids and metal salts. *Environ. Pollut.* **159**, 1523–1535.

Bourgeault A., Ciffroy P., Garnier C., Cossu-Leguille C., Masfaraud J. F., Charlatchka R. and Garnier J. M. (2013) Speciation and bioavailability of dissolved copper in different freshwaters: Comparison of modelling, biological and chemical responses in aquatic mosses and gammarids. *Sci. Total Environ.* **452**–**453**, 68–77.

Bowman R. A. and Focht D. D. (1974) The influence of glucose and nitrate concentrations upon denitrification rates in sandy soils. *Soil Biol. Biochem.* **6**, 297–301.

Brown K., Tegoni M., Prudêncio M., Pereira A. S., Besson S., Moura J. J., Moura I. and Cambillau C. (2000) A novel type of catalytic copper cluster in nitrous oxide reductase. *Nat. Struct. Biol.* **7**, 191–195.

Bruland K. W., Rue E. L., Donat J. R., Skrabal S. A. and Moffett J. W. (2000) Intercomparison of voltammetric techniques to determine the chemical speciation of dissolved copper in a coastal

667 seawater sample. *Anal. Chim. Acta* **405**, 99–113.
668 Buchwald C., Grabb K., Hansel C. M. and Wankel S. D. (2016) Constraining the role of iron in
669 environmental nitrogen transformations: Dual stable isotope systematics of abiotic NO_2^- reduction
670 by Fe(II) and its production of N_2O. *Geochim. Cosmochim. Acta* **186**, 1–12.
671 Burgin A. J. and Hamilton S. K. (2007) Have we overemphasized the role of denitrification in aquatic
672 ecosystems? A review of nitrate removal pathways. *Front. Ecol. Environ.* **5**, 89–96.
673 Campana O., Simpson S. L., Spadaro D. A. and Blasco J. (2012) Sub-lethal effects of copper to benthic
674 invertebrates explained by sediment properties and dietary exposure. *Environ. Sci. Technol.* **46**,
675 6835–6842.
676 Di Capua F., Pirozzi F., Lens P. N. L. and Esposito G. (2019) Electron donors for autotrophic
677 denitrification. *Chem. Eng. J.* **362**, 922–937.
678 Carreira C., Nunes R. F., Mestre O., Moura I. and Pauleta S. R. (2020) The effect of pH on Marinobacter
679 hydrocarbonoclasticus denitrification pathway and nitrous oxide reductase. *J. Biol. Inorg. Chem.* **25**,
680 927–940.
681 Castaldelli G., Colombani N., Soana E., Vincenzi F., Fano E. A. and Mastrocicco M. (2019) Reactive
682 nitrogen losses via denitrification assessed in saturated agricultural soils. *Geoderma* **337**, 91–98.
683 Chakraborty P., Ramteke D. and Chakraborty S. (2015) Geochemical partitioning of Cu and Ni in
684 mangrove sediments: Relationships with their bioavailability. *Mar. Pollut. Bull.* **93**, 194–201.
685 Chen D., Yuan X., Zhao W., Luo X., Li F. and Liu T. (2020) Chemodenitrification by Fe(II) and nitrite:
686 pH effect, mineralization and kinetic modeling. *Chem. Geol.* **541**, 119586.
687 Clement J. C., Shrestha J., Ehrenfeld J. G. and Jaffe P. R. (2005) Ammonium oxidation coupled to
688 dissimilatory reduction of iron under anaerobic conditions in wetland soils. *Soil Biol. Biochem.* **37**,
689 2323–2328.
690 Davidson E. A., Chorover J. and Dail D. B. (2003) A mechanism of abiotic immobilization of nitrate in
691 forest ecosystems: The ferrous wheel hypothesis. *Glob. Chang. Biol.* **9**, 228–236.
692 Doane T. A. (2017) The Abiotic Nitrogen Cycle. *ACS Earth Sp. Chem.* **1**, 411–421.
693 Doroski A. A., Helton A. M. and Vadas T. M. (2019) Greenhouse gas fluxes from coastal wetlands at the
694 intersection of urban pollution and saltwater intrusion: A soil core experiment. *Soil Biol. Biochem.*
695 **131**, 44–53.
696 Fu M. H. and Tabatabai M. A. (1989) Nitrate reductase activity in soils: Effects of trace elements. *Soil*
697 *Biol. Biochem.* **21**, 943–946.
698 Fulda B., Voegelin A., Ehlert K. and Kretzschmar R. (2013a) Redox transformation, solid phase
699 speciation and solution dynamics of copper during soil reduction and reoxidation as affected by
700 sulfate availability. *Geochim. Cosmochim. Acta* **123**, 385–402.

Fulda B., Voegelin A., Maurer F., Christl I. and Kretzschmar R. (2013b) Copper redox transformation and complexation by reduced and oxidized soil humic acid. 1. X-ray absorption spectroscopy study. *Environ. Sci. Technol.* **47**, 10903–10911.

Giannopoulos G., Hartop K. R., Brown B. L., Song B., Elsgaard L. and Franklin R. B. (2020) Trace metal availability affects greenhouse gas emissions and microbial functional group abundance in freshwater wetland sediments. *Front. Microbiol.* **11**, 1–12.

Glass J. B. and Orphan V. J. (2012) Trace metal requirements for microbial enzymes involved in the production and consumption of methane and nitrous oxide. *Front. Microbiol.* **3**, 1–20.

Godden A. J. W., Turley S., Teller D. C., Adman E. T., Liu M. Y., Payne W. J. and Legall J. (1991) The 2.3 angstrom X-Ray structure of nitrite reductase from Achromobacter cycloclastes. *Science (80-.).* **253**, 438–442.

Granger J. and Ward B. B. (2003) Accumulation of nitrogen oxides in copper-limited cultures of denitrifying bacteria. *Limnol. Oceanogr.* **48**, 313–318.

Han S., Zhang Y., Masunaga S., Zhou S. and Naito W. (2014) Relating metal bioavailability to risk assessment for aquatic species: Daliao River watershed, China. *Environ. Pollut.* **189**, 215–222.

Huang S. and Wang Z. (2003) Application of anodic stripping voltammetry to predict the bioavailable/toxic concentration of Cu in natural water. *Appl. Geochemistry* **18**, 1215–1223.

Huffman S. A. and Barbarick K. A. (1981) Soil nitrate analysis by cadmium reduction. *Commun. Soil Sci. Plant Anal.* **12**, 79–89.

IPCC (2014) Climate Change 2014: Impacts, Adaptation, and Vulnerability. Contribution of Working Group II to the Fifth Assessment Report of the Intergovernmental Panel on Climate Change.

Iwasaki H., Saigo T. and Matsubara T. (1980) Copper as a controlling factor of anaerobic growth under N_2O and biosynthesis of N_2O reductase in denitrifying bacteria. *Plant Cell Physiol.* **21**, 1573–1584.

Jacinthe P. A. and Tedesco L. P. (2009) Impact of elevated copper on the rate and gaseous products of denitrification in freshwater sediments. *J. Environ. Qual.* **38**, 1183–1192.

Jormakka M., Richardson D., Byrne B. and Iwata S. (2004) Architecture of NarGH reveals a structural classification of Mo-bisMGD enzymes. *Structure* **12**, 95–104.

Kleber M. and Lehmann J. (2019) Humic substances extracted by alkali are invalid proxies for the dynamics and functions of organic matter in terrestrial and aquatic ecosystems. *J. Environ. Qual.* **48**, 207–216.

Klueglein N., Zeitvogel F., Stierhof Y. D., Floetenmeyer M., Konhauser K. O., Kappler A. and Obst M. (2014) Potential role of nitrite for abiotic Fe(II) oxidation and cell encrustation during nitrate reduction by denitrifying bacteria. *Appl. Environ. Microbiol.* **80**, 1051–1061.

Knowles R. (1982) Denitrification. *Microbiol. Rev.* **46**, 43–70.

Koponen H. T., Flojt L. and Martikainen P. J. (2004) Nitrous oxide emissions from agricultural soils at low temperatures: A laboratory microcosm study. *Soil Biol. Biochem.* **36**, 757–766.

Kozelka P. B. and Bruland K. W. (1998) Chemical speciation of dissolved Cu, Zn, Cd, Pb in Narragansett Bay, Rhode Island. *Mar. Chem.* **60**, 267–282.

Kremen A., Bear J., Shavit U. and Shaviv A. (2005) Model demonstrating the potential for coupled nitrification denitrification in soil aggregates. *Environ. Sci. Technol.* **39**, 4180–4188.

Krom M. D. (1980) Spectrophotometric determination of ammonia: a study of a modified Berthelot reaction using salicylate and dichloroisocyanurate. *Analyst* **105**, 305–316.

Kurdi F. and Donner H. E. (1983) Zinc and copper sorption and interaction in soils. *Soil Sci. Soc. Am. J.* **47**, 873–876.

Du Laing G., Rinklebe J., Vandecasteele B., Meers E. and Tack F. M. G. (2009) Trace metal behaviour in estuarine and riverine floodplain soils and sediments: A review. *Sci. Total Environ.* **407**, 3972–3985.

Liu R., Ma T., Zhang D., Lin C. and Chen J. (2020) Spatial distribution and factors influencing the different forms of ammonium in sediments and pore water of the aquitard along the Tongshun River, China. *Environ. Pollut.* **266**, 115212.

Liu T., Chen D., Luo X., Li X. and Li F. (2019) Microbially mediated nitrate-reducing Fe(II) oxidation: Quantification of chemodenitrification and biological reactions. *Geochim. Cosmochim. Acta* **256**, 97–115.

Magalhaes C., Costa J., Teixeira C. and Bordalo A. A. (2007) Impact of trace metals on denitrification in estuarine sediments of the Douro River estuary , Portugal. **107**, 332–341.

Makowski D. (2019) N_2O increasing faster than expected. *Nat. Clim. Chang.* **9**, 909–910.

Marschner B. and Kalbitz K. (2003) Controls of bioavailability and biodegradability of dissolved organic matter in soils. *Geoderma* **113**, 211–235.

Martinez-Espinosa C., Sauvage S., Al Bitar A., Green P. A., Vorosmarty C. J. and Sanchez-Perez J. M. (2021) Denitrification in wetlands: A review towards a quantification at global scale. *Sci. Total Environ.* **754**.

Matocha C. J., Dhakal P. and Pyzola S. M. (2012) The role of abiotic and coupled biotic/abiotic mineral controlled redox processes in nitrate reduction. *Adv. Agron.* **115**, 181–214.

Matus F., Stock S., Eschenbach W., Dyckmans J., Merino C., Nájera F., Köster M., Kuzyakov Y. and Dippold M. A. (2019) Ferrous Wheel Hypothesis: Abiotic nitrate incorporation into dissolved organic matter. *Geochim. Cosmochim. Acta* **245**, 514–524.

Mehlhorn J., Besold J., Lezama Pacheco J. S., Gustafsson J. P., Kretzschmar R. and Planer-Friedrich B. (2018) Copper mobilization and immobilization along an organic matter and redox gradient - insights from a mofette Site. *Environ. Sci. Technol.* **52**, 13698–13707.

769 Melton E. D., Swanner E. D., Behrens S., Schmidt C. and Kappler A. (2014) The interplay of microbially
770 mediated and abiotic reactions in the biogeochemical Fe cycle. *Nat. Rev. Microbiol.* **12**, 797–808.
771 Merill L. and Tonjes D. J. (2014) A review of the hyporheic zone, stream restoration, and means to
772 enhance denitrification. *Crit. Rev. Environ. Sci. Technol.* **44**, 2337–2379.
773 Milne C. J., Kinniburgh D. G., Van Riemsdijk W. H. and Tipping E. (2003) Generic NICA - Donnan
774 model parameters for metal-ion binding by humic substances. *Environ. Sci. Technol.* **37**, 958–971.
775 Milne C. J., Kinniburgh D. G. and Tipping E. (2001) Generic NICA-Donnan model parameters for proton
776 binding by humic substances. *Environ. Sci. Technol.* **35**, 2049–2059.
777 Moraghan J. T. and Buresh R. J. (1977) Chemical reduction of nitrite and nitrous oxide by ferrous iron.
778 *Soil Sci. Soc. Am. J.* **41**, 47–50.
779 Mwagona P. C., Yao Y., Yuanqi S. and Yu H. (2019) Laboratory study on nitrate removal and nitrous
780 oxide emission in intact soil columns collected from nitrogenous loaded riparian wetland, Northeast
781 China. *PLoS One* **14**, 1–21.
782 Myneni S. C. B. (2019) Chemistry of natural organic matter—The next step: commentary on a humic
783 substances debate. *J. Environ. Qual.* **48**, 233–235.
784 Nag S. K., Liu R. and Lal R. (2017) Emission of greenhouse gases and soil carbon sequestration in a
785 riparian marsh wetland in central Ohio. **189**, 1–12.
786 Nano G. V. and Strathmann T. J. (2006) Ferrous iron sorption by hydrous metal oxides. *J. Colloid*
787 *Interface Sci.* **297**, 443–454.
788 Nojiri M., Xie Y., Inoue T., Yamamoto T., Matsumura H., Kataoka K., Deligeer, Yamaguchi K., Kai Y.
789 and Suzuki S. (2007) Structure and function of a hexameric copper-containing nitrite reductase.
790 *Proc. Natl. Acad. Sci. U. S. A.* **104**, 4315–4320.
791 Nowicki B. L. (1994) The effect of temperature, oxygen, salinity, and nutrient enrichment on estuarine
792 denitrification rates measured with a modified nitrogen gas flux technique. *Estuar. Coast. Shelf Sci.*
793 **38**, 137–156.
794 Ochoa-Herrera V., León G., Banihani Q., Field J. A. and Sierra-Alvarez R. (2011) Toxicity of copper(II)
795 ions to microorganisms in biological wastewater treatment systems. *Sci. Total Environ.* **412**–**413**,
796 380–385.
797 Otte J. M., Blackwell N., Ruser R., Kappler A., Kleindienst S. and Schmidt C. (2019) N_2O formation by
798 nitrite-induced (chemo)denitrification in coastal marine sediment. *Sci. Rep.* **9**, 10691.
799 Ottley C. J., Davison W. and Edmunds W. M. (1997) Chemical catalysis of nitrate reduction by iron(II).
800 *Geochim. Cosmochim. Acta* **61**, 1819–1828.
801 Pan Y., Ye L., Ni B. J. and Yuan Z. (2012) Effect of pH on N_2O reduction and accumulation during
802 denitrification by methanol utilizing denitrifiers. *Water Res.* **46**, 4832–4840.

Pansu M. and Gautheyrou J. (2006) Handbook of soil analysis: Mineralogical, organic and inorganic methods. In *Springer, Berlin Heidelberg.*

Peters B., Casciotti K. L., Samarkin V. A., Madigan M. T., Schutte C. A. and Joye S. B. (2014) Stable isotope analyses of NO_2^-, NO_3^-, and N_2O in the hypersaline ponds and soils of the McMurdo Dry Valleys, Antarctica. *Geochim. Cosmochim. Acta* **135**, 87–101.

Ponthieu M., Pourret O., Marin B., Schneider A. R., Morvan X., Conreux A. and Cancès B. (2016) Evaluation of the impact of organic matter composition on metal speciation in calcareous soil solution: Comparison of Model VI and NICA-Donnan. *J. Geochemical Explor.* **165**, 1–7.

Rahman M. M., Roberts K. L., Grace M. R., Kessler A. J. and Cook P. L. M. (2019) Role of organic carbon, nitrate and ferrous iron on the partitioning between denitrification and DNRA in constructed stormwater urban wetlands. *Sci. Total Environ.* **666**, 608–617.

Ren Z. L., Tella M., Bravin M. N., Comans R. N. J., Dai J., Garnier J. M., Sivry Y., Doelsch E., Straathof A. and Benedetti M. F. (2015) Effect of dissolved organic matter composition on metal speciation in soil solutions. *Chem. Geol.* **398**, 61–69.

Robertson E. K. and Thamdrup B. (2017) The fate of nitrogen is linked to iron(II) availability in a freshwater lake sediment. *Geochim. Cosmochim. Acta* **205**, 84–99.

Robinson T. C., Latta D. E., Notini L., Schilling K. E. and Scherer M. M. (2021) Abiotic reduction of nitrite by Fe(II): a comparison of rates and N_2O production . *Environ. Sci. Process. Impacts* **23**, 1531–1541.

Rudnick R. L. and Gao S. (2003) Composition of the continental crust. *The crust* **3**, 1–64.

Sakadevan K., Zheng H. and Bavor H. J. (1999) Impact of heavy metals on denitrification in surface wetland sediments receiving wastewater. *Water Sci. Technol.* **40**, 349–355.

Sander R. (2015) Compilation of Henry's law constants (version 4.0) for water as solvent. *Atmos. Chem. Phys.* **15**, 4399–4981.

Schmidt F., Koch B. P., Goldhammer T., Elvert M., Witt M., Lin Y. S., Wendt J., Zabel M., Heuer V. B. and Hinrichs K. U. (2017) Unraveling signatures of biogeochemical processes and the depositional setting in the molecular composition of pore water DOM across different marine environments. *Geochim. Cosmochim. Acta* **207**, 57–80.

Schultz C. and Grundl T. (2004) pH Dependence of ferrous sorption onto two smectite clays. *Chemosphere* **57**, 1301–1306.

Shaaban M., Peng Q. an, Bashir S., Wu Y., Younas A., Xu X., Rashti M. R., Abid M., Zafar-ul-Hye M., Núñez-Delgado A., Horwath W. R., Jiang Y., Lin S. and Hu R. (2019) Restoring effect of soil acidity and Cu on N_2O emissions from an acidic soil. *J. Environ. Manage.* **250**, 109535.

Shampine L. F., Gladwell I. and Thompson S. (2003) *Solving ODEs with MATLAB*. Cambridge university

837 press.
838 Shen W., Xue H., Gao N., Shiratori Y., Kamiya T., Fujiwara T., Isobe K. and Senoo K. (2020) Effects of
839 copper on nitrous oxide (N_2O) reduction in denitrifiers and N_2O emissions from agricultural soils.
840 *Biol. Fertil. Soils* **56**, 39–51.
841 Simek M. and Cooper J. E. (2002) The influence of soil pH on denitrification: Progress towards the
842 understanding of this interaction over the last 50 years. *Eur. J. Soil Sci.* **53**, 345–354.
843 Skrabal S. A., Donat J. R. and Burdige D. J. (2000) Pore water distributions of dissolved copper and
844 copper-complexing ligands in estuarine and coastal marine sediments. *Geochim. Cosmochim. Acta*
845 **64**, 1843–1857.
846 Sovacool B. K., Griffiths S., Kim J. and Bazilian M. (2021) Climate change and industrial F-gases: A
847 critical and systematic review of developments, sociotechnical systems and policy options for
848 reducing synthetic greenhouse gas emissions. *Renew. Sustain. Energy Rev.* **141**, 110759.
849 Sparks D. L., Page A. L., Helmke P. A., Loeppert R. H., Soltanpour P. N., Tabatabai M. A., Johnston C.
850 T. and Sumner M. E. (1996) Methods of soil analysis. Part 3: Chemical Methods. In *Soil Science*
851 *Society of America, Madison.*
852 Stumm W. and Sulzberger B. (1992) The cycling of iron in natural environments: Considerations based
853 on laboratory studies of heterogeneous redox processes. *Geochim. Cosmochim. Acta* **56**, 3233–3257.
854 Su J. F., Luo X. X., Wei L., Ma F., Zheng S. C. and Shao S. C. (2016) Performance and microbial
855 communities of Mn(II)-based autotrophic denitrification in a Moving Bed Biofilm Reactor (MBBR).
856 *Bioresour. Technol.* **211**, 743–750.
857 Su J. F., Zheng S. C., Huang T. L., Ma F., Shao S. C., Yang S. F. and Zhang L. N. (2015)
858 Characterization of the anaerobic denitrification bacterium Acinetobacter sp. SZ28 and its
859 application for groundwater treatment. *Bioresour. Technol.* **192**, 654–659.
860 Tian H., Chen G., Lu C., Xu X., Ren W., Zhang B., Banger K., Tao B., Pan S., Liu M., Zhang C.,
861 Bruhwiler L. and Wofsy S. (2015) Global methane and nitrous oxide emissions from terrestrial
862 ecosystems due to multiple environmental changes. *Ecosyst. Heal. Sustain.* **1**, 1–20.
863 Tian H., Xu R., Canadell J. G., Thompson R. L., Winiwarter W., Suntharalingam P., Davidson E. A.,
864 Ciais P., Jackson R. B., Janssens-Maenhout G., Prather M. J., Regnier P., Pan N., Pan S., Peters G.
865 P., Shi H., Tubiello F. N., Zaehle S., Zhou F., Arneth A., Battaglia G., Berthet S., Bopp L.,
866 Bouwman A. F., Buitenhuis E. T., Chang J., Chipperfield M. P., Dangal S. R. S., Dlugokencky E.,
867 Elkins J. W., Eyre B. D., Fu B., Hall B., Ito A., Joos F., Krummel P. B., Landolfi A., Laruelle G. G.,
868 Lauerwald R., Li W., Lienert S., Maavara T., MacLeod M., Millet D. B., Olin S., Patra P. K., Prinn
869 R. G., Raymond P. A., Ruiz D. J., van der Werf G. R., Vuichard N., Wang J., Weiss R. F., Wells K.
870 C., Wilson C., Yang J. and Yao Y. (2020) A comprehensive quantification of global nitrous oxide

sources and sinks. *Nature* **586**, 248–256.

Traina S. J. and Doner H. E. (1985) Heavy metal induced releases of manganese (II) from a hydrous manganese dioxide. *Soil Sci. Soc. Am. J.* **49**, 317–321.

Twining B. S., Mylon S. E. and Benoit G. (2007) Potential role of copper availability in nitrous oxide accumulation in a temperate lake. *Limnol. Oceanogr.* **52**, 1354–1366.

Wang J., Wang S., Jin X., Zhu S. and Wu F. (2008) Ammonium release characteristics of the sediments from the shallow lakes in the middle and lower reaches of Yangtze River region, China. *Environ. Geol.* **55**, 37–45.

Wang M., Hu R., Zhao J., Kuzyakov Y. and Liu S. (2016) Iron oxidation affects nitrous oxide emissions via donating electrons to denitrification in paddy soils. *Geoderma* **271**, 173–180.

Wang S., Pi Y., Jiang Y., Pan H., Wang Xiaoxia, Wang Xiaomin, Zhou J. and Zhu G. (2020) Nitrate reduction in the reed rhizosphere of a riparian zone: From functional genes to activity and contribution. *Environ. Res.* **180**, 108867.

Wang Z., Jiang Y., Awasthi M. K., Wang J., Yang X., Amjad A., Wang Q., Lahori A. H. and Zhang Z. (2018) Nitrate removal by combined heterotrophic and autotrophic denitrification processes: Impact of coexistent ions. *Bioresour. Technol.* **250**, 838–845.

Waska H., Brumsack H. J., Massmann G., Koschinsky A., Schnetger B., Simon H. and Dittmar T. (2019) Inorganic and organic iron and copper species of the subterranean estuary: Origins and fate. *Geochim. Cosmochim. Acta* **259**, 211–232.

Weber K. A., Urrutia M. M., Churchill P. F., Kukkadapu R. K. and Roden E. E. (2006) Anaerobic redox cycling of iron by freshwater sediment microorganisms. *Environ. Microbiol.* **8**, 100–113.

Wei J., Ibraim E., Brüggemann N., Vereecken H. and Mohn J. (2019) First real-time isotopic characterisation of N_2O from chemodenitrification. *Geochim. Cosmochim. Acta* **267**, 17–32.

Xu J., Tan W., Xiong J., Wang M., Fang L. and Koopal L. K. (2016) Copper binding to soil fulvic and humic acids: NICA-Donnan modeling and conditional affinity spectra. *J. Colloid Interface Sci.* **473**, 141–151.

Yan J., Flynn E., Sharma N., Giammar D., Schwartz G., Brooks S., Weisenhorn P., Kemner K., O'Loughlin E., Kaplan D. and Catalano J. (2021) Consistent Controls on Trace Metal Micronutrient Speciation in Wetland Soils and Stream Sediments. *Geochim. Cosmochim. Acta*. Available at: https://doi.org/10.1016/j.gca.2021.10.017.

Yan M. and Korshin G. V. (2014) Comparative examination of effects of binding of different metals on chromophores of dissolved organic matter. *Environ. Sci. Technol.* **48**, 3177–3185.

Yuan X., Pham A. N., Xing G., Rose A. L. and Waite T. D. (2012) Effects of pH, chloride, and bicarbonate on Cu(I) oxidation kinetics at circumneutral pH. *Environ. Sci. Technol.* **46**, 1527–1535.

Zhang C., Yu Z. G., Zeng G. M., Jiang M., Yang Z. Z., Cui F., Zhu M. Y., Shen L. Q. and Hu L. (2014) Effects of sediment geochemical properties on heavy metal bioavailability. *Environ. Int.* **73**, 270–281.

Zhao L., Dong H., Edelmann R. E., Zeng Q. and Agrawal A. (2017) Coupling of Fe(II) oxidation in illite with nitrate reduction and its role in clay mineral transformation. *Geochim. Cosmochim. Acta* **200**, 353–366.

Zhao L., Dong H., Kukkadapu R., Agrawal A., Liu D., Zhang J. and Edelmann R. E. (2013) Biological oxidation of Fe(II) in reduced nontronite coupled with nitrate reduction by Pseudogulbenkiania sp. Strain 2002. *Geochim. Cosmochim. Acta* **119**, 231–247.

Zhao S., Su X., Wang Y., Yang X., Bi M., He Q. and Chen Y. (2020) Copper oxide nanoparticles inhibited denitrifying enzymes and electron transport system activities to influence soil denitrification and N_2O emission. *Chemosphere* **245**, 125394.

Zhu-Barker X., Cavazos A. R., Ostrom N. E., Horwath W. R. and Glass J. B. (2015) The importance of abiotic reactions for nitrous oxide production. *Biogeochemistry* **126**, 251–267.

Zhu I. and Getting T. (2012) A review of nitrate reduction using inorganic materials. *Environ. Technol. Rev.* **1**, 46–58.

Zhu Y. and Elzinga E. J. (2014) Formation of layered Fe(II)-hydroxides during Fe(II) sorption onto clay and metal-oxide substrates. *Environ. Sci. Technol.* **48**, 4937–4945.

Zhu Y., Jin X., Tang W., Meng X. and Shan B. (2019) Comprehensive analysis of nitrogen distributions and ammonia nitrogen release fluxes in the sediments of Baiyangdian Lake, China. *J. Environ. Sci. (China)* **76**, 319–328.

Figures and Tables

Table 1: Cu loadings used for conducting incubation experiments, and dissolved Cu concentrations in the fluid after equilibration

Site	Control		Low loading		High loading	
	Cu added (µmol/g)	Dissolved conc. (nM)	Cu added (µmol/g)	Dissolved conc. (nM)	Cu added (µmol/g)	Dissolved conc. (nM)
Riparian 1	N.A	29±10	0.25	280±60	1.3	2300±500
Riparian 2	N.A	41±9	0.25	97±10	2.5	560±40
Stream 1	N.A	3±1	0.25	16±2	2.5	53±7
Stream 2	N.A	6±2	0.50	52±6	5.0	590±30
Marsh 1	N.A	48±5	0.13	290±10	0.63	1400±100

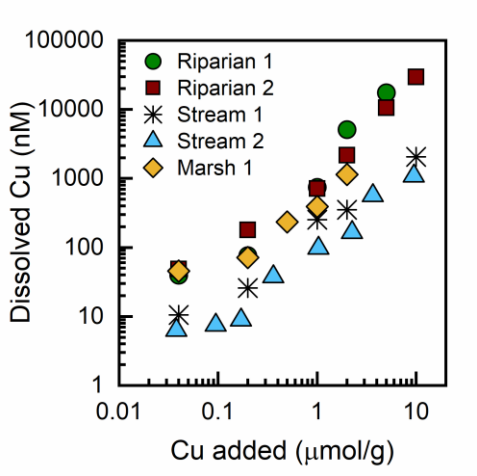

Figure 1: Experimentally determined values of Cu uptake by wetland soils and stream sediments, for use in determining Cu loading in microcosm experiments. Here, Riparian 2 and Riparian 1 represent selected locations from the riparian wetland soil, Marsh 1 from marsh wetland soil, and Stream 2 and Stream 1 are locations from a stream sediment site.

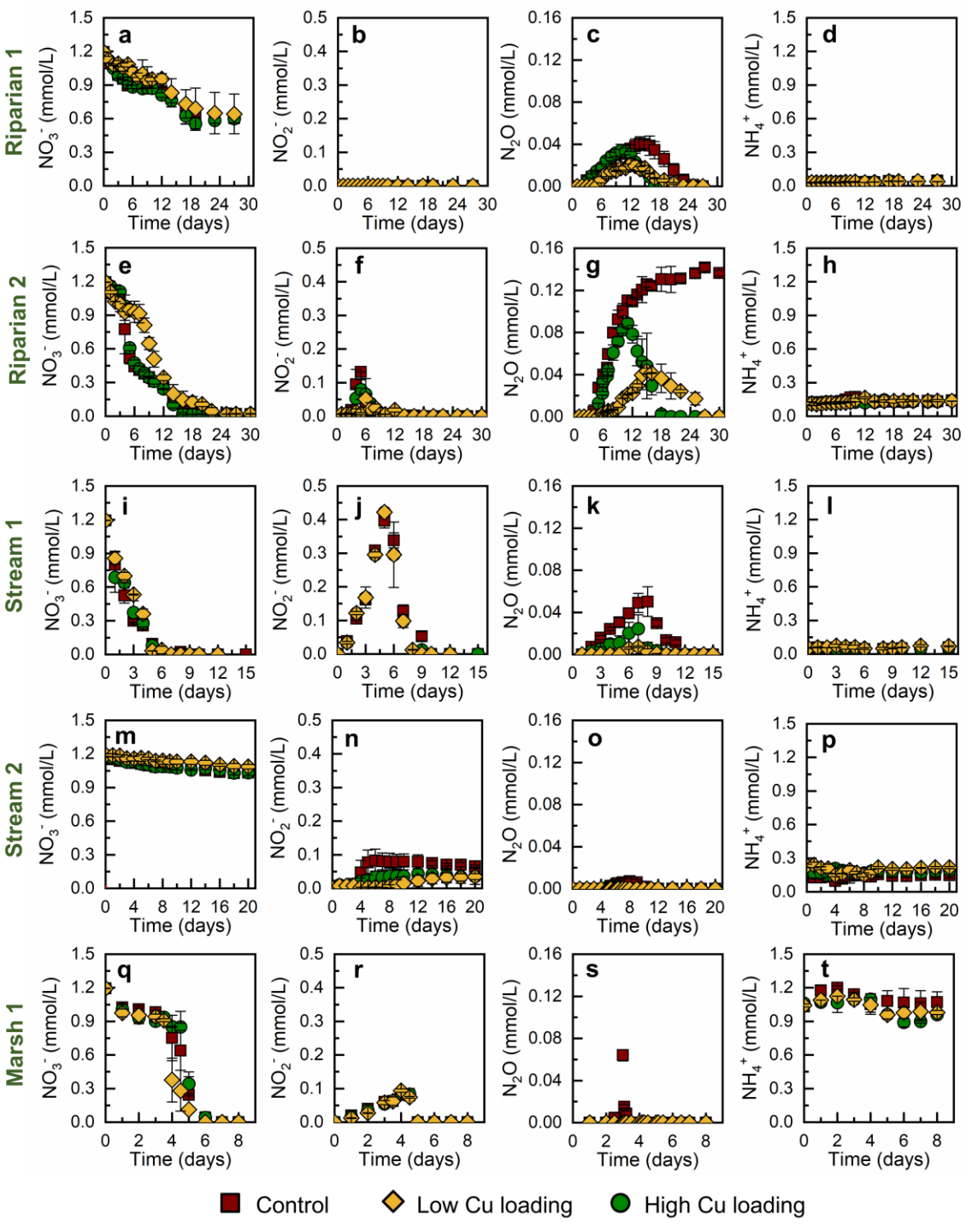

Figure 2: Variation in the concentrations of different N- species (mmol-N L^{-1}) during the incubation experiments for (a-d) Riparian 1, (e-h) Riparian 2, (i-l) Stream 1, (m-p) Stream 2 and (q-t) Marsh 1. In case of low Cu loading, 0.25 µmol/g Cu was added in incubation experiments for Riparian 1, Riparian 2, and Stream 1 samples, 0.50 µmol/g for Steam 2 and 0.13 µmol/g for Marsh 1 incubations. High Cu loading amendments for incubation experiments were 5.0 µmol/g for Riparian 1 and Stream 1, 1.3 µmol/g for Riparian 2, 5.0 µmol/g for Stream 2, and 0.63 µmol/g for Marsh 1.

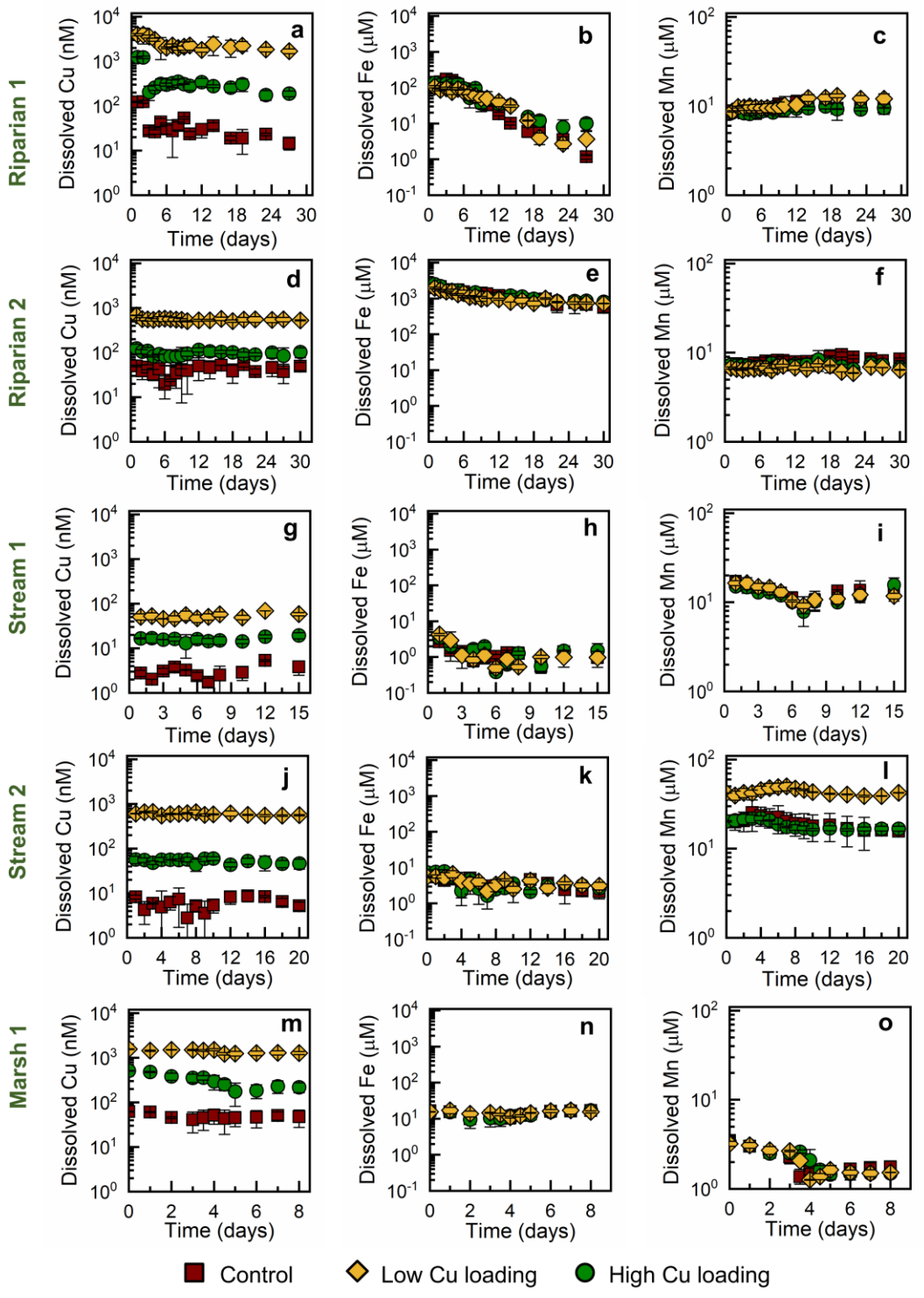

Figure 3: Variation in the concentrations of Cu, Fe and Mn during the incubation experiments for (a-c) Riparian 2, (d-f) Riparian 1, (g-i) Stream 1, (j-l) Stream 2 and (m-o) Marsh 1. In case of low Cu loading, 0.25 µmol/g Cu was added in incubation experiments for Riparian 1, Riparian 2, and Stream 1 samples, 0.50 µmol/g for Steam 2 and 0.13 µmol/g for Marsh 1 incubations. High Cu loading amendments for incubation experiments were 5.0 µmol/g for Riparian 1 and Stream 1, 1.3 µmol/g for Riparian 2, 5.0 µmol/g for Stream 2, and 0.63 µmol/g for Marsh 1.

Table 2: The values of Michaelis-Menten parameters of different reactions involved in carrying out denitrification at different sites as well as the pseudo first-order rate constant for abiotic reduction of NO_2^- to N_2.

Site	Condition	V_{max} (mmol L^{-1} day^{-1})	$K_{NO_3^-}$ (mmol L^{-1})	k_{ab} (day^{-1})	$K_{NO_2^-}$ (mmol L^{-1})	K_{N_2O} (mmol L^{-1})
Riparian 1	Control	0.41	12	99	0.072	6900
	Low loading	0.41	11	99	0.072	24
	High loading	0.41	15	98	0.068	3.5
Riparian 2	Control	0.25	1.1	2.2	0.68	11000
	Low loading	0.25	1.1	2.2	0.22	0.48
	High loading	0.25	1.7	2.2	0.33	0.21
Stream 1	Control	0.39	0.39	0.69	9.1	3.7
	Low loading	0.39	0.41	0.71	9.7	0.72
	High loading	0.39	0.49	0.64	9.5	0.00078
Stream 2	Control	0.37	39	0.015	0.079	0.008
	Low loading	0.37	40	0.015	0.0067	0.002
	High loading	0.37	71	0.015	0.0035	0.003
Marsh 1	Control	0.27	0.47	0.0002	0.058	0.14
	Low loading	0.27	0.55	0.0002	0.067	0.037
	High loading	0.27	0.38	0.0002	0.047	0.018

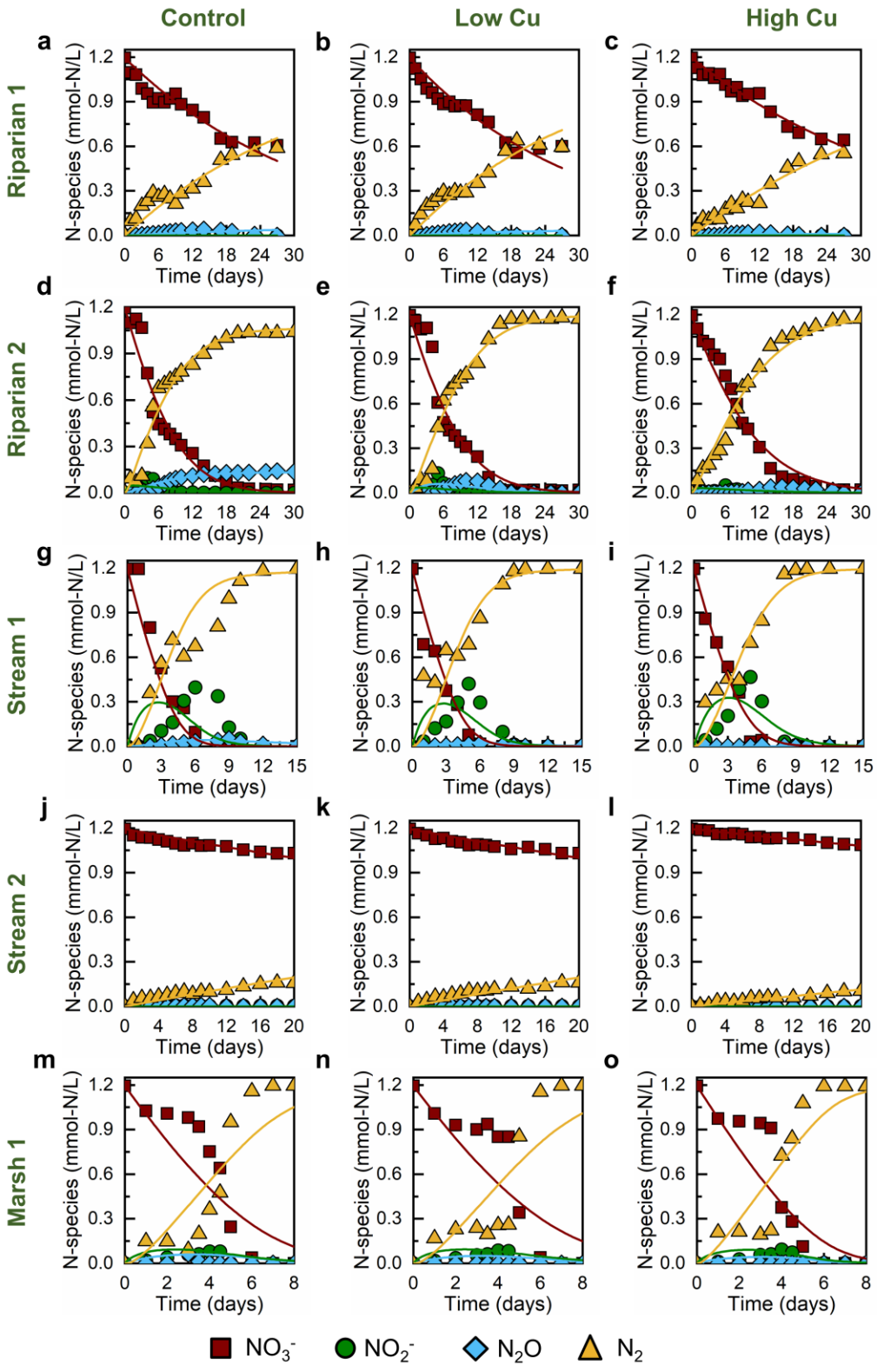

Figure 4: Experimental data together with the output of the optimized kinetic model for the evolution of N-containing species during the incubation experiments using the parameters obtained from the kinetic model for (a-c) Riparian 1, (d-f) Riparian 2, (g-i) Stream 1, (j-l) Stream 2 and (m-o) Marsh 1

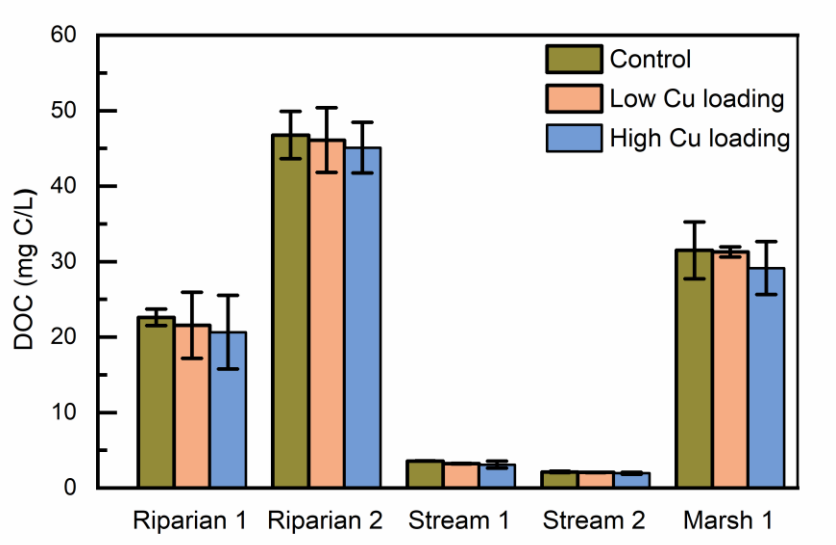

Figure 5: Final dissolved organic carbon concentrations in the incubation experiments with soils and sediments of different natural aquatic systems.

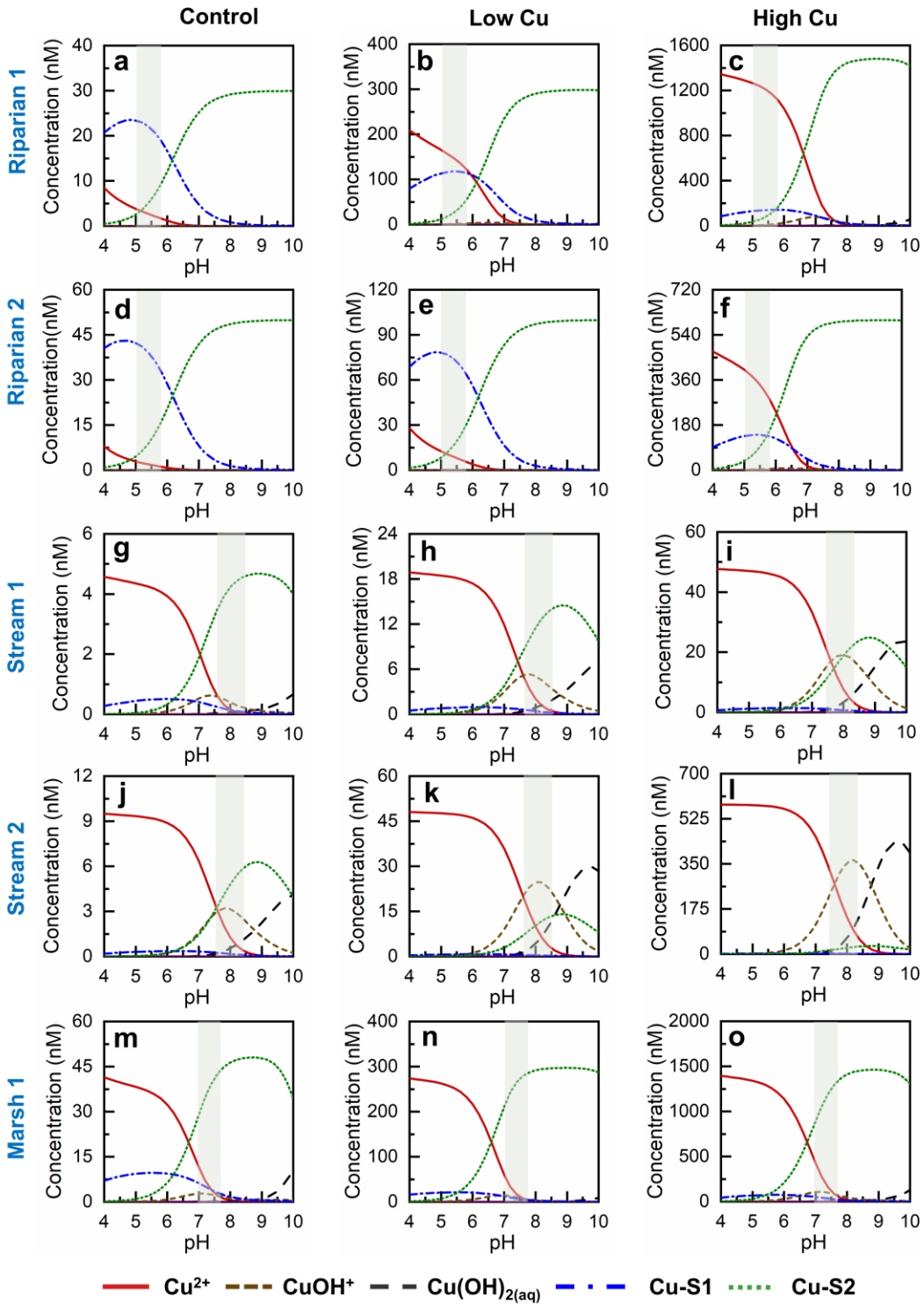

Figure 6: Speciation of dissolved Cu at different concentrations for (a-c) Riparian 2 (d-f) Riparian 1 and (g-i) Stream 2 (j-l) Stream 2 and (m-o) Marsh 1. The concentrations of Cu selected for determining the speciation are based on the dissolved concentration of Cu in the incubation experiments (Table 1). Here, Cu-S1 shows Cu bound to carboxylic acids of organic carbon and Cu-S2 is the Cu bound to phenolic groups on organic carbon. Shaded areas indicate the pH range over the course of the experiment.

SUPPLEMENTARY MATERIAL FOR

Copper availability governs nitrous oxide accumulation in wetland soils and stream sediments

Neha Sharma,[1] Elaine D. Flynn,[2] Jeffrey G. Catalano[2] and Daniel E. Giammar[1]

[1]*Department of Energy, Environmental and Chemical Engineering, Washington University in St. Louis, St. Louis, Missouri 63130, United States*

[2]*Department of Earth and Planetary Sciences, Washington University in St. Louis, St. Louis, Missouri 63130, United States*

*Corresponding Author:

Address: Department of Energy, Environmental and Chemical Engineering, Washington University in St. Louis, St. Louis, MO 63130, USA

Phone: (314) 935-6849

Email: giammar@wustl.edu\

submitted to *Geochimica et Cosmochimica Acta*

Supplementary material details

Table S1: Concentration of major elements and species in the simulated site water used for uptake studies and microcosm experiments

Parameter	ANL	ORNL	TB
pH	7.0	7.6	5.0
Ionic Strength	1.7 mM	7.0 mM	0.30 mM
	Concentration (µM)		
Na^+	170	450	60
K^+	170	71	5.3
Ca^{2+}	370	1100	25
Mg^{2+}	290	390	27
Cl-	490	2700	160
SO_4^{2-}	580	260	7.6
NO_3^-	8	70	0
NH_4^+	0	0.2	0
PO_4^{3-}	0	4	0

Table S2: Characterization of soils and sediments collected from different aquatic systems (Yan et al.)

Site	Cu (nmol/g)	Mn (nmol/g)	Fe (µmol/g)	C (%)	S (%)	NH_4^+ (µmol/g)	NO_2^- (µmol/g)	NO_3^- (µmol /g)
Riparian 1	48	220	47	1.3	0.02	1.1	BDL	0.14
Riparian 2	260	701	460	6.0	0.09	2.7	BDL	0.00
Stream 1	160	3200	204	3.0	0.10	2.7	BDL	0.14
Stream 2	98	5600	420	0.46	0.02	2.8	BDL	0.43
Marsh 1	280	1960	420	9.0	0.24	21	BDL	0.36

Here, nutrients represent the extractable values from soils and sediments. Total Cu, Mn, and Fe concentrations present in soils and sediments were obtained using microwave-assisted digestion technique. Carbon and sulfur percent were estimated using CHNS analyzer. The detection limit of NO_2^- is 0.02 µmol/g.

Section S1: Dissolved Cu speciation in microcosms

Two different binding sites are considered in the NICA model, type 1 and type 2, corresponding to carboxylic (low affinity) and phenolic (high affinity) sites respectively (Benedetti et al., 1995).

$$Q_i = \frac{n_{i,1}}{n_{H,1}} Q_{\max 1,H} \frac{(\acute{K}_{i,1} c_i)^{n_{i,1}}}{\sum(\acute{K}_{i,1} c_i)^{n_{i,1}}} \frac{\left[\sum(\acute{K}_{i,1} c_i)^{n_{i,1}}\right]^{p_1}}{1+\left[\sum(\acute{K}_{i,1} c_i)^{n_{i,1}}\right]^{p_1}} + \frac{n_{i,2}}{n_{H,2}} Q_{\max 1,H} \frac{(\acute{K}_{i,2} c_i)^{n_{i,2}}}{\sum(\acute{K}_{i,2} c_i)^{n_{i,2}}} \frac{\left[\sum(\acute{K}_{i,1} c_i)^{n_{i,2}}\right]^{p_2}}{1+\left[\sum(\acute{K}_{i,1} c_i)^{n_{i,2}}\right]^{p_2}} \quad \text{Eq S1}$$

where, c_i (mol. L-1) is the concentration of metal; Q_i is the amount of bound ion described by two identical binding expressions, one each for the carboxylic- (1) and phenolic-type (2) site distributions. $Q_{max1,H}$ and $Q_{max2,H}$ are the maximum proton binding capacity of humic substances within each distribution (mol kg^{-1}); p_1 and p_2 account for intrinsic heterogeneity of humic substances; $\acute{K}_{i,1}$ and $\acute{K}_{i,2}$ are median values for affinity distributions for ion, and $n_{i,1}$ and $n_{i,2}$ are used to describe the nonidealities of the ion-binding to each distribution. The ratios $\frac{n_{i,j}}{n_{H,j}}$ with j = 1 or 2 reflect the average stoichiometry of ion binding.

The charge on humic substances is neutralized by the nonspecific binding of counter-ions and exclusion of co-ions within the Donnan volume, V_D ($L \cdot kg^{-1}$), as described by the empirical relationship.

$$logV_D = b(1 - logI) - 1 \quad \text{Eq S2}$$

Here, I is ionic strength and b is an empirical parameter describing the variation of Donnan volume with ionic strength (Benedetti et al., 1996). The values of parameters used in estimating Cu speciation are listed in Table S3.

Humic substances are normally assumed to be the main binding substances (Ren et al., 2015), and their concentrations were determined from the dissolved organic carbon (DOC) concentrations. Humic substances account for 60% of DOC in natural water systems (Zhang and Davison, 2000; Gueguen et al., 2011), and they comprise 50% carbon, so concentration of HS was assumed to be 1.2 times the DOC concentration. The pH, temperature, total dissolved elements (Na, Mg, K, Ca, Cl, NO_3, SO_4, and PO_4) (Table EA1), and dissolved Cu, Fe, and Mn were used as the input parameters for determining Cu speciation.

Table S3: Parameters used in NICA-Donnan model for determining Cu speciation in the presence of DOC (Xu et al., 2016)

Parameter	Value
b	0.57
$Q_{\max 1,H}$	5.88
p_1	0.59
$log\acute{k}_{H,1}$	2.34
$n_{H,1}$	0.66
$log\acute{k}_{Cu,1}$	0.26
$n_{Cu,1}$	0.53
$Q_{\max 2,H}$	1.86
p_2	0.70
$log\acute{k}_{H,2}$	8.60
$n_{H,2}$	0.76
$log\acute{k}_{Cu,2}$	8.26
$n_{Cu,2}$	0.36

.

Table S4: Estimated labile concentrations of Cu in the microcosms using NICA-Donnan model

Site	Estimated labile concentration (nM)*		
	Control	Low Cu	High Cu
Riparian 1	2.8 ± 0.9	150 ± 20	1200 ± 80
Riparian 2	1.4 ± 0.8	8.9 ± 3	350 ± 60
Stream 1	0.55 ± 0.3	7.2 ± 2	28 ± 4
Stream 2	4.8 ± 0.9	38 ± 3	560 ± 4
Marsh 1	7.6 ± 5	35 ± 30	150 ± 100

*Labile Cu concentration is the sum of Cu, $CuOH^+$, and $Cu(OH)_2$. The values represent the average of the labile concentrations between the pH range studied. pH varied between 5-6 in wetland soils; 7.6-8.6 in stream sediments, and 7-8 in marsh wetland soils.

Section S2: Estimation of organic carbon requirements for complete reduction of nitrate

$$\mathbf{CH_2O + H_2O \rightarrow CO_2 + 4e^- + 4H^+} \quad \text{Eq S3}$$

$$\mathbf{NO_3^- + 5e^- + 6H^+ \rightarrow \frac{1}{2} N_2 + 3H_2O} \quad \text{Eq S4}$$

$$\mathbf{5CH_2O + 4H^+ + 4NO_3^- \rightarrow 5CO_2 + 2N_2 + 7H_2O} \quad \text{Eq S5}$$

Total nitrate available=0.05 mmol

Total organic carbon (OC) requirement = 0.0625 mmol

Site	**Organic Carbon (%)**	**Total organic carbon (mmol)**	$\frac{TOC}{OC_{required}}$
Riparian 2	6.0	13	208
Riparian 1	1.3	2.7	43
Stream 1	3.1	6.3	101
Stream 2	0.46	0.77	12
Marsh 1	9.0	19	304

*Here, total organic carbon represents the total amount of organic carbon present in the solid phase (2.5 g of soil/sediment) used for incubation experiments.

Section S3: Estimation of nitrate requirements for abiotic reaction with Fe(II)

$$NO_3^- + 5Fe^{2+} + 12H_2O \rightarrow \frac{1}{2}N_{2(g)} + 5Fe(OH)_3 + 9H^+$$

Riparian 1:

Decrease in Fe : 7.1 µmol

NO_3^- required: 1.4 µmol

Riparian 2:

Decrease in Fe concentration: 72 µmol

NO_3^- required: 14 µmol

Stream 1:

Decrease in Fe concentration: 0.084 µmol

NO_3^- required: 0.017 µmol

References

Benedetti M. F., Milne C. J., Kinniburgh D. G., Van Riemsdijk W. H. and Koopal L. K. (1995) Metal ion binding to humic substances: Application of the non-ideal competitive adsorption model. *Environ. Sci. Technol.* **29**, 446–457.

Benedetti M. F., Van Riemsdijk W. H. and Koopal L. K. (1996) Humic substances considered as a heterogeneous Donnan gel phase. *Environ. Sci. Technol.* **30**, 1805–1813.

Gueguen C., Clarisse O., Perroud A. and McDonald A. (2011) Chemical speciation and partitioning of trace metals (Cd, Co, Cu, Ni, Pb) in the lower Athabasca river and its tributaries (Alberta, Canada). *J. Environ. Monit.* **13**, 2865–2872.

Ren Z. L., Tella M., Bravin M. N., Comans R. N. J., Dai J., Garnier J. M., Sivry Y., Doelsch E., Straathof A. and Benedetti M. F. (2015) Effect of dissolved organic matter composition on metal speciation in soil solutions. *Chem. Geol.* **398**, 61–69.

Xu J., Tan W., Xiong J., Wang M., Fang L. and Koopal L. K. (2016) Copper binding to soil fulvic and humic acids: NICA-Donnan modeling and conditional affinity spectra. *J. Colloid Interface Sci.* **473**, 141–151.

Zhang H. and Davison W. (2000) Direct in situ measurements of labile inorganic and organically bound metal species in synthetic solutions and natural waters using diffusive gradients in thin films. *Anal. Chem.* **72**, 4447–4457.